DESIGN AND ANALYSIS OF A FEW WIDEBAND ANTENNAS FOR WLAN / WiMAX APPLICATIONS

THESIS SUBMITTED IN PARTIAL FULFILLMENT OF THE REQUIREMENT FOR THE DEGREE OF

MASTER OF ENGINEERING
IN
ELECTRONICS AND TELE-COMMUNICATION ENGINEERING

THESIS SUBMITTED BY

SAYAN SARKAR

University Registration No: 140689 of 2017-2018

Exam Roll No: M4ETC19006

Class Roll No: 001710702002

UNDER THE GUIDANCE OF

PROFESSOR BHASKAR GUPTA

DEPARTMENT OF ELECTRONICS AND TELE-COMMUNICATION ENGINEERING

JADAVPUR UNIVERSITY

KOLKATA – 700032

INDIA

FACULTY OF ENGINEERING AND TECHNOLOGY
ELECTRONICS AND TELECOMMUNICATION ENGINEERING
JADAVPUR UNIVERSITY

CERTIFICATE OF RECOMMENDATION

This is to certify that the thesis entitled "**DESIGN AND ANALYSIS OF A FEW WIDEBAND ANTENNAS FOR WLAN / WiMAX APPLICATIONS**" has been carried out by **SAYAN SARKAR** (***University Registration No: 140689 of 2017-2018***) under my guidance and supervision and be accepted in partial fulfilment of the requirement for awarding the degree of "**MASTER OF ENGINEERING IN ELECTRONICS and TELE COMMUNICATION ENGINEERING**". The research results presented in this thesis have not been included in any other paper submitted for the award of any degree to any other Institute or University

---

PROFESSOR BHASKAR GUPTA

THESIS SUPERVISOR

DEPT. OF ELECTRONICS AND TELECOMMUNICATION ENGINEERING
JADAVPUR UNIVERSITY
KOLKATA 700032

PROF. SHELI SINHA CHAUDHURI

HEAD OF THE DEPARTMENT

DEPT. OF ELECTRONICS AND TELECOMMUNICATION ENGINEERING

JADAVPUR UNIVERSITY
KOLKATA 700032

PROF. CHIRANJIB BHATTACHARJEE

DEAN

FACULTY OF ENGINEERING AND TECHNOLOGY

JADAVPUR UNIVERSITY
KOLKATA 700032

FACULTY OF ENGINEERING AND TECHNOLOGY
ELECTRONICS AND TELECOMMUNICATION ENGINEERING
JADAVPUR UNIVERSITY

CERTIFICATE OF APPROVAL[#]

The foregoing THESIS is hereby approved as a creditable study of an Engineering Subject carried out and presented in a manner of satisfactory to warrant its acceptance as a pre-requisite to the DEGREE for which it has been submitted. It is to be understood that by this approval, the undersigned do not necessarily endorse or approve any statement made, opinion expressed or conclusion drawn therein but approve the THESIS only for the purpose for which it has been submitted.

Committee on final examination
for the evaluation of the Thesis

_____
(Signature of the Supervisor)

_____
(Signature of the Examiner)

only in case the thesis is approved.

FACULTY OF ENGINEERING AND TECHNOLOGY
ELECTRONICS AND TELECOMMUNICATION ENGINEERING
JADAVPUR UNIVERSITY

DECLARATION OF ORIGINALITY AND COMPLIANCE OF ACADEMIC ETHICS

I hereby declare that this thesis contains literature survey and original research work done by the undersigned candidate, as a part of his degree of "**MASTER OF ENGINEERING IN ELECTRONICS AND TELE-COMMUNICATION ENGINEERING".** All information in this document has been obtained and presented in accordance with academic rules and ethical conduct. I also declare that as required by these rules and conduct, I have fully cited and referenced all materials and results that are not original to this work.

Thesis Title

DESIGN AND ANALYSIS OF A FEW WIDEBAND ANTENNAS FOR WLAN / WiMAX APPLICATIONS

SAYAN SARKAR

University Registration No: 140689 of 2017-2018

Exam Roll No: M4ETC19006

Class Roll No: 001710702002

DEPT. OF ELECTRONICS AND TELECOMMUNICATION ENGINEERING

JADAVPUR UNIVERSITY

KOLKATA – 700032

INDIA

Date: _____ _____

(SAYAN SARKAR)

ACKNOWLEDGEMENT

Firstly, I wish to take this opportunity to thank my Master's supervisor Professor Bhaskar Gupta and acknowledge the deep impact he has had in cultivating within me the interest and curiosity that I have developed towards the theory and applications of Electromagnetism of which Microwave Engineering is but a small part. His patience, the immense knowledge he shares with us and the relationship he has with all his students clearly brings out the best in them. I am very thankful that I have been able to work under the guidance of such an able and well established professor.

I would like to thank Dr. Sudhabindu Ray for all his comments and discussions which have very often helped clear many of my doubts and helped me look at things from a different perspective. I also wish to express my gratitude to the previous head of the department, Prof. Palaniandavar Venkateswaran and the current head of the department Prof. Sheli Sinha Chaudhuri for always extending a helping hand whenever needed and giving me the opportunity of attending conferences where I could bring myself up to speed with the latest research in the various fields of Electromagnetics.

This thesis would not have been complete without the help and co operation of all my seniors of JU Microwave Lab who took the time and effort to help me immensely with all my fabrications and engage in very knowledgeable discourse which helped me learn a plethora of things regarding my subject that I was previously unaware of.

Lastly, but most importantly, I would like to thank my father and mother for encouraging me to pursue the subject I love and for their constant and unwavering faith in my abilities. Without their support, I would definitely not be where I am today.

Date: _____ _____

(SAYAN SARKAR)

CONTENTS

CHAPTER - I

INTRODUCTION

1.1 PREFACE

In the 21st century, digital information is one of the biggest resources worldwide. Information has become more valuable than assets like oil and money. With the whole world connected through the internet, the power of information has never been more significant. With the increase in significance of information, the methods of communicating this information has also improved by leaps and bounds over the past several decades with intensive research being pursued throughout the world to improve the existing systems to cater to the needs of the millions connected worldwide.

Wireless communication is one of the most advanced forms of communication and also the most popular and beneficial form for long distance information exchange. One of the major components of wireless communication is the antenna, which acts as a transponder and converts the electrical signal containing the information to an electromagnetic wave which can propagate through free space following the equations of James Clerk Maxwell who did pioneering work in the field of electromagnetism and for the first time unified electricity, magnetism and light as different manifestations of the same phenomenon in the 1860s [1],[2]. The antennas at the receiver and the transmitter play a major part in determining how efficiently and how far the signal will propagate and how well it will be received. Therefore, a lot of wireless communication research revolves around the modification and betterment of the antenna systems used.

Most communication systems carry out wireless communications in the specified IEEE wireless communication standard channels. The IEEE 802 standard is used for Local Area Networks (LAN) and Metropolitan Area Networks (MAN) [3]. Within this standard, the IEEE 802.11 and the 802.16 are used for Wireless Local Area Networks (WLANs) and Worldwide Interoperability for Microwave Access (WiMAX) respectively. Since these two standards are extensively used worldwide, a lot of research has been focused on antennas operating in these bands with the aim of creating more efficient systems.

1.2 OBJECTIVE OF THE THESIS

As mentioned in the previous section, the IEEE 802 standard is very important for communication systems. Within the 802.11 group, the most commonly used frequency bands include the 2.4 GHz band (IEEE 802.11 b/g/n/ax) and the 5 GHz band (IEEE 802.11 a/j/n/ax) [4] which are more commonly called the WLAN bands. The 802.16 group is used mainly for WiMAX and includes the 3.5 GHz band (IEEE 802.16 d/e) [5].

This thesis mainly focuses on the design and analysis of a few antenna structures which can be used in the above mentioned frequency bands.

Initially, a literature review is carried out on the various antennas already designed and working in the WLAN and WiMAX regions. Then, a few antennas capable of working within these frequency bands are designed and studied. All the designed antennas presented in this thesis are different in some aspects from antennas found in previous literature.

The analysis of the designed antenna structures has been carried out using CST Studio Suite® which is a full wave EM simulation software. The various simulated antenna parameters are extracted and studied. Most of the designed antenna structures (except the Alphabet Shaped Antennas analyzed using Characteristic Mode theory in Chapter 6) have also been fabricated and the various resulting antenna parameters have been measured. Comparisons between the simulated and measured parameters are presented in each of these cases which serve to highlight the similarities and dissimilarities between the simulated data and the practical data obtained. The fabricated antennas are all wideband in nature and can easily be used with existing communication systems for information transfer in the WLAN and/or WiMAX bands.

1.3 ORGANIZATION OF THE THESIS

The thesis has been divided into 7 chapters.

The 1st chapter (the current one) gives a brief introduction of the work carried out and the objective of the work.

The 2nd chapter deals with the literature review which provided the basis for carrying out the research.

The 3rd chapter is about the design and analysis of *A Balanced Feed Triple Frequency Patch Loaded Printed Dipole Antenna for WiMAX/WLAN Applications*. The antenna has been fabricated and measured results are presented along with the simulated ones.

The 4th chapter contains a study on the *Effects of two different modified ground planes on an equilateral triangular ring shaped patch antenna.* The two antennas have also been fabricated and experimental verifications are carried out.

The 5th chapter deals with the design and analysis of *A star shaped wideband patch antenna with central circular slot for WLAN and WiMAX applications.* The fabricated structure along with the measured data is presented.

The 6th chapter is dedicated to the *Characteristic Mode Analysis of a few Symmetric English Alphabet Shaped Antennas*. The Characteristic Mode Theory for Perfect Electric Conducting bodies is used to analyze a few English alphabet shaped antennas and determine where they might radiate along with their surface currents distributions, electric field distributions, magnetic field distributions as well as the far field radiation patterns. The antenna dimensions are so chosen that they have radiating modes in the WLAN and/or WiMAX frequency regions. However this analysis and study is only simulation based and none of the designed antennas have been fabricated.

The 7th chapter provides the conclusion of this thesis.

REFERENCES

[1] https://en.wikipedia.org/wiki/James_Clerk_Maxwell#cite_ref-ADTEF_7-1

[2] *Maxwell, James Clerk (1865). "A dynamical theory of the electromagnetic field*". *Philosophical Transactions of the Royal Society of London.* ***155****: 459-512.* (This article accompanied an 8 December 1864 presentation by Maxwell to the Royal Society. His statement that "light and magnetism are affections of the same substance" is at page 499.)

[3] http://www.ieee802.org/

[4] https://en.wikipedia.org/wiki/IEEE_802.11

[5] https://www.electronics-notes.com/articles/connectivity/wimax/frequencies-spectrum-bands.php

CHAPTER - II

LITERATURE REVIEW

2.1 PREFACE

This chapter highlights some of the previous works done in the selected areas of the thesis. The chapter is divided into four parts.

The 1st part corresponds to the literature review done for chapter 3, i.e. *A Balanced Feed Triple Frequency Patch Loaded Printed Dipole Antenna for WiMAX/WLAN Applications*.

The 2nd part corresponds to the literature review done for chapter 4, i.e. *Effects of two different modified ground planes on an equilateral triangular ring shaped patch antenna.*

The 3rd part corresponds to the literature review done for chapter 5, i.e. *A star shaped wideband patch antenna with central circular slot for WLAN and WiMAX applications.*

Finally, the 4th part consists of literature review corresponding to chapter 6, i.e. *Characteristic Mode Analysis of a few Symmetric English Alphabet Shaped Antennas.*

2.2 LITERATURE REVIEW IN PARTS

2.2.1 A BALANCED FEED TRIPLE FREQUENCY PATCH LOADED PRINTED DIPOLE ANTENNA FOR WIMAX/WLAN APPLICATIONS.

Dipole and monopole antennas are some of the most commonly used and popular antennas for wireless communication systems worldwide. While physicist Heinrich Hertz was the first person to use a dipole antenna to demonstrate the existence of radio waves in 1887, Guglielmo Marconi empirically found that he could just ground the transmitter (or one side of a transmission line, if used) dispensing with one half of the antenna, thus realizing the vertical or monopole antenna (sometime in 1895) [1].

Based on the pioneering works of Hertz and Marconi, numerous variants of the dipole and monopole antenna have been designed, modified and studied. The

main advantage of monopole and dipole antennas lies in the fact that they possess omnidirectional radiation patterns in the plane perpendicular to the wire axis (the azimuth plane for vertical antennas). The radiation patterns appear as toroids (doughnut shaped) and are symmetric about the wires [2].

A planar variant of the wire dipole is the printed dipole. In this case, the dipole structure is made planar similar to a microstrip patch antenna, sitting on top of a substrate. A very good description about the working and operation of printed dipoles and their comparisons with microstrip dipoles is given in [3]. The advantage of printed dipoles is the fact that they can easily be integrated with other components within portable handheld devices and are almost similar in nature to their wire counterparts. Therefore printed dipoles are much more popular while designing compact integrated circuits.

A uniplanar bowtie shaped printed dipole antenna has been presented in [4] while it was modified by the same authors in [5] to enhance the VSWR =2 bandwidth. The double-sided bowtie antenna element was used to develop a monopulse dipole array [6] and a printed circuit cylindrical array antenna [7].

Dipole antennas, printed or wired, are balanced antennas and therefore need balanced feeds. Therefore, feeds for printed dipole antennas include Coplanar Strips (CPS) and baluns which convert unbalanced feeds to balanced ones. The printed version of a parallel two-wire line, called a parallel strip line was analyzed by Wheeler [8]. An integrated microstrip balun has been investigated in [9], which follows the theory of a coaxial balun structure proposed in [10], [11].

In [12], authors have demonstrated a triple-frequency antenna for sub-GHz wireless communication, whereas the authors of [13] have presented a triple band antenna for WLAN/WiMAX applications within a short range. In [14], the authors have reported a planar tri-band antenna for access points of WLAN/Wi-Fi.

Following this literature review, the proposed printed dipole antenna was designed and fabricated with an integrated balun to convert the unbalanced microstrip feed to a balanced one for the dipole input. The antenna was designed with dimensions which ensure that it radiates in the WiMAX and WLAN region with wideband characteristics.

2.2.2 Effects of two different modified ground planes on an equilateral triangular ring shaped patch antenna.

Triangular patch antennas have been studied extensively both theoretically and practically. They are smaller in size and provide more or less same radiation characteristics as their rectangular counterparts. A good description of the resonant frequencies, various modes and field distributions of triangular patch antennas is given in [15]. Similar to a nearly square patch, a nearly equilateral can produce circular polarization. [16], [17], [18].

Ring-shaped microstrip antennas have been studied as alternatives to the conventional patch structures. Rectangular rings, triangular rings as well as circular ring patch antennas have been studied. Resonant rings are usually smaller in size than their corresponding counterparts and depend on the width of the microstrip used [19]. The mean circumference of the ring generally equals the guided wavelength of the microstrip used.

Triangular ring slot antennas have been designed and studied in [20]. Simple triangular rings have also been presented in [21], [22] whereby they are used as dual/triple frequency radiators with dual/ triple polarizations. A similar structure consisting of triangular ring antennas for dual-frequency dual polarization or circular polarization operations is also presented in [23].

However all the above references have full ground planes and none have studied the effects of modified ground planes on triangular ring antennas. Radiating ground planes have been studied in [24] where notches have been developed on the ground plane to help it radiate.

The equilateral-triangular ring shaped antennas are designed with two different modified ground planes to find out their effects on the radiation characteristics of the antenna. The antennas are simulated and fabricated and simulated as well as measured results are presented.

2.2.3. A STAR SHAPED WIDEBAND PATCH ANTENNA WITH CENTRAL CIRCULAR SLOT FOR WLAN AND WIMAX APPLICATIONS.

With the increase in demand for higher bandwidth for faster and larger amounts of data transfer, wideband antenna design has gained a lot of importance. The designed antennas must also be small and compact so that they can be efficiently integrated within small portable handheld devices.

Another major requirement for portable antennas is an omnidirectional radiation pattern which helps them carry out data transfer along the azimuth plane (for vertically placed antennas) with equal intensity in all directions.

Wideband antennas can be designed by removing part or most of the ground plane of a microstrip patch antenna to allow for more permissible radiation modes to occur naturally as well as to provide an omnidirectional radiation pattern for the structure. Proper impedance matching of such structures leads to very wideband antennas which are omnidirectional throughout most of the -10dB reflection coefficient bandwidth [25].

Literature is reviewed to find some such wideband antennas useful for WiMAX/ WLAN applications. A dual band printed folded dipole antenna is presented in [26] for 2.45 GHz and 3.5 GHz applications. However, the antenna is large in size and also directional at 3.5 GHz. A printed broadband monopole antenna for WLAN/WiMAX is presented in [27]. But the antenna is again large in size, has low gain and very low efficiency. A dual band antenna is presented in [28] but it has numerous parameters which need optimization and careful designing.

A reconfigurable multiband antenna is presented for WiFi, WiMAX and WLAN applications [29] but it has a large area (2400 mm^2). In [30], a compact wideband open-end slot antenna is presented but it has relatively large size as well. Coplanar bowtie antenna [31] and a broadband antenna for WiMAX and WLAN [32] are also relatively large in size. Wideband antennas presented in [33], [34] are also not omnidirectional in all the required frequencies.

A star-shaped antenna is designed in the thesis which is smaller in size than all the above referred designs and which also provides omnidirectional patterns at the frequencies of requirement. The antenna is fabricated and the measured results are also presented.

2.2.4. Characteristic Mode Analysis of a few Symmetric English Alphabet Shaped Antennas.

Characteristic Mode Analysis (CMA) can predict the various inherent modal characteristics of a structure and are independent of any external sources or excitations. Characteristic Modes can be defined as a particular set of surface currents and radiated fields that are the characteristics of the obstacle/ body under consideration.

The Characteristic Mode Theory was first derived by R. J. Garbacz in 1968 [35]. It was later modified by Garbacz and Turpin [36]. Harrington and Mautz [37], [38] derived a different method of obtaining the Characteristic Modes which proved to be much simpler and more efficient to perform considering the types of problems at hand. The theory of Characteristic Modes for Perfect Electric Conducting bodies, dielectric bodies, and multilayered bodies has been described with great detail and examples in [39].

CM analysis provides a great tool for analyzing Electromagnetic structures to find out the various different properties that the body possesses. It can be used to design antennas and analyze the inherent characteristics of the antenna coupled with most of the parameters which decide whether it can work as an efficient radiator at the desired design frequency.

In this thesis, some English Alphabet Shaped antennas are designed using CST Studio Suite and analysed using Characteristic Mode Theory for Perfect Electric Conducting Bodies (PECs).

The results of the analysis are provided and it is seen that the chosen dimensions of the alphabets result in making the antennas efficient radiators in the WLAN and/or WiMAX frequency regions. No fabrications are made, only simulation analysis of the alphabet shaped antennas is done in this thesis.

REFERENCES

[1] Constantine A. Balanis, *Modern Antenna Handbook* , 2011, John Wiley and Sons. pp. 2–1. ISBN 1118209753.

[2] Constantine A. Balanis, *Antenna Theory: Analysis and Design (3rd Ed.), 2005*, Wiley-Interscience, pp. 151-204, ISBN 9780471667827, 047166782X.

[3] P. Bhartia, Inder Bahl, R. Garg, A. Ittipiboon, *Microstrip Antenna Design Handbook*, 2000, Artech House Publishers, pp. 399-425, ISBN 0890065136, 9780890065136.

[4] Lin, Y.-D., and S.-N. Tsai, "Coplanar Waveguide-Fed Uniplanar Bow-Tie Antenna," *IEEE Trans. on Antennas and Propagation*, Vol. AP-45, 1997, pp.305-306.

[5] Lin, Y.-D., and S.-N. Tsai, "Analysis and Design of Broadside-Coupled Striplines-Fed Bow-Tie Antennas," *IEEE Trans. on Antennas and Propagation*, Vol. AP-46, 1998, pp.459-460.

[6] Agarwal, A.K., and W.E, Powell, "Monopulse Printed Circuit Dipole Array,' *IEEE Trans. on Antennas and Propagation*, Vol. AP-33, 1985, pp. 1280-1283.

[7] Agarwal, A.K., and W.E, Powell, "A Printed Circuit Cylindrical Array Antenna,' *IEEE Trans. on Antennas and Propagation*, Vol. AP-34, 1986, pp. 1288-1293.

[8] Wheeler, H.A., "Transmission Line Properties of Parallel Strips Separated by a Dielectric Sheet,' *IEEE Trans. on Microwave Theory and Techniques*, Vol. MTT-13, 1965, pp. 172-185.

[9] D. Edward and D. Rees, "A broadband printed dipole with integrated balun," Microwave Journal, pp. 339-344, May 1987.

[10] W. K. Roberts, "A new wide band balun," Proceedings of the IRE, vol. 45, pp. 1628-1631, Dec. 1957.

[11] G. Oltman, "The compensated balun," IEEE Trans. Microwave Theory Tech., Vol. 14, pp. 1628-1631, Mar. 1966.

[12] S. Genovesi, A. Monorchio and S. Saponara, "Compact triple-frequency antenna for sub-GHz wireless communications," IEEE Antennas and Wireless Propagation Letters, Vol. 11, pp. 14-17, 2012.

[13] K. George Thomas and M. Sreenivasan, "A novel triple band printed antenna for WLAN/WiMAX applications," Microwave and Optical Technology Letters, Vol. 51, No. 10, pp. 2481-2485, October 2009

[14] R.L. Li, X.L. Quan, Y.H. Cui and M.M. Tentzeris, "Directional triple-band planar antenna for WLAN/WiMax access points," Electronics Letters., pp. 305-306, 15th March 2012 Vol. 48 No. 6

[15] P. Bhartia, Inder Bahl, R. Garg, A. Ittipiboon, *Microstrip Antenna Design Handbook*, 2000, Artech House Publishers, pp. 425-435, ISBN 0890065136, 9780890065136.

[16] Suzuki, Y., N. Miyano and T. Chiba, "Circularly Polarised Radiation from Singly Fed Equilateral- Triangular Microstrip Antenna," *Proc. IEEE,* Vol. 134, Pt. H, 1987, pp. 194-198.

[17] Lu, J.-H., C.-L. Tang, and K.-L., Wong, "Circular Polarization Design of a Single-Feed Equilateral- Triangular Microstrip Antenna," *Electron. Let.*Vol.34, 1998, pp. 319-321.

[18] Lu, J.-H., C.-L. Tang, and K.-L., Wong, "Single-Feed Slotted Equilateral- Triangular Microstrip Antenna for Circular Polarization," *IEEE Trans. on Antennas and Propagation*, Vol. AP-47, 1999, pp. 1174-1178.

[19] P. Bhartia, Inder Bahl, R. Garg, A. Ittipiboon, *Microstrip Antenna Design Handbook*, 2000, Artech House Publishers, pp. 366-391, ISBN 0890065136, 9780890065136.

[20] Jin-Sen Chen, "Studies of CPW-fed equilateral triangular-ring slot antennas and triangular-ring slot coupled patch antennas," IEEE transactions on Antennas and Propagation, Vol. 53, No. 7, July 2005, pp. 2208-2211.

[21] Linli Jiang ,Chunlan Lu ,Wenquan Cao ,Changsong Wu ,Feng Yuan, "A dual-band and dual polarized antenna with two nested triangular rings," 2017 Sixth Asia-Pacific Conference on Antennas and Propagation (APCAP), 2017, pp. 1-3.

[22] Tao Zhang, Wei Hong, Ke Wu, "A low-profile triple-band triple-polarization antenna with two triangular rings," IEEE transactions on Antennas and Propagation, Vol.14, 2015, pp. 378-381.

[23] Tao Zhang, Yan Zhang, Wei Hong, and KeWu, "Triangular Ring Antennas for Dual-Frequency Dual-Polarization or Circular-Polarization Operations," IEEE ANTENNAS AND WIRELESS PROPAGATION LETTERS, VOL. 13, 2014, pp. 971-974.

[24] M. Cabedo-Fabres ; E. Antonino-Daviu ; A. Valero-Nogueira ; M. Ferrando-Bataller, "Wideband radiating ground plane with notches," 2005 IEEE Antennas and Propagation Society International Symposium, Vol. 2B, 2005, pp. 560-563.

[25] Daniel Valderas, Juan Ignacio Sancho, David Puente, Cong Ling, Xiaodong Chen, *ULTRAWIDEBAND ANTENNAS: Design and Applications,*2011, Imperial College Press, pp. 157-165, ISBN-13 978-1-84816-491-8 ,10 1-84816-491-2.

[26] B. H. Ahmad, H. Nornikman," Dual band printed folded dipole antenna for wireless communication at 2.4 GHz and 3.5 GHz applications," 2015 Asia-Pacific Microwave Conference (APMC), 2015, Vol.3, pp.1-3.

[27] I-Fong Chen, Chia-MeiPeng," Printed broadband monopole antenna for WLAN/WiMAX Applications," IEEE Antennas and Wireless Propagation Letters, 2009, Vol.8, pp. 472-474.

[28] Linli Jiang ,Chunlan Lu ,Wenquan Cao ,Changsong Wu ,Feng Yuan, "A dual-band and dual polarized antenna with two nested triangular rings," 2017 Sixth Asia-Pacific Conference on Antennas and Propagation (APCAP), 2017, pp. 1-3.

[29] Ali MANSOUL, "Reconfigurable Multiband Bowtie Antenna for WiFi, WiMax, and WLAN Applications," 2017 IEEE International Symposium on Antennas and Propagation & USNC/URSI National Radio Science Meeting, 2017, pp. 1147-1148.

[30] Zhe-Jun Jin and Tae-Yeoul Yun, "Compact Wideband Open-End Slot Antenna With Inherent Matching," IEEE ANTENNAS AND WIRELESS PROPAGATION LETTERS, VOL. 13, 2014, pp. 1385-1388.

[31] Qing-Le Zhang, Li-Ming Si, Yu-Ming Wu, Yong Liu, and Xin Lv, "Design of a Coplanar Bowtie Antenna for WLAN and WiMAX Application," 2014 3rd Asia-Pacific Conference on Antennas and Propagation, 2014, pp. 284-286.

[32] M.A Matin, M.P Saha, H. M. Hasan, "Design of Broadband Patch Antenna for WiMAX and WLAN," 2010 International Conference on Microwave and Millimeter Wave Technology, 2010, pp. 1-3.

[33] Fayyadh H. Ahmed and Bayez K. Alsulaifanie, "Dual-Wideband Printed Rectangular Monopole Antenna for Wireless Applications," 2014 Loughborough Antennas and Propagation Conference (LAPC), 2014, pp. 576-579.

[34] Chien-Yuan Pan, Tzyy-Sheng Horng, Wen-Shan Chen and Chien-Hsiang Huang, "Dual Wideband Printed Monopole Antenna for WLAN/WiMAX Applications," IEEE ANTENNAS AND WIRELESS PROPAGATION LETTERS, VOL. 6, 2007, pp. 149-151.

[35] R. J. Garbacz, "A Generalized Expansion for Radiated and Scattered Fields," Ph.D. dissertation, Ohio State University, Columbus, 1968

[36] R . J. Garbacz and R. H. Turpin, "A generalized expansion for radiated and scattered fields," IEEE Trans. Antennas Propagation, vol. AP - 19, no. 3, pp. 348–358, May 1971.

[37] R. F. Harrington and J. R. Mautz, "Theory of Characteristic Modes for Conducting Bodies," IEEE Trans. Antennas Propagation, vol. AP-19, no. 5, pp. 622- 628, Sept. 1971.

[38] R. F. Harrington and J. R. Mautz, "Computation of Characteristic Modes for Conducting Bodies," IEEE Trans. Antennas Propagation, vol. AP-19, no. 5, pp. 629- 639, Sept. 1971.

[39] Yikai Chen, Chao-Fu Wang, *Characteristic Modes: Theory and Applications in Antenna Engineering*, John Wiley and Sons, 2015, ISBN: 1119038421, 9781119038429.

CHAPTER - III

A BALANCED FEED TRIPLE FREQUENCY PATCH LOADED PRINTED DIPOLE ANTENNA FOR WIMAX/WLAN APPLICATIONS

3.1 INTRODUCTION

The advent of wireless communication combined with planar antenna design has brought about a revolution in the modern world. Today there are countless antenna systems which cater to the wireless needs of millions worldwide.

With the increase in number of portable electronics and communication gadgets, the need for smaller and compact planar antennas has also increased. Antennas required for communication usually need to be omnidirectional at least at some of the required frequency regions. Omnidirectionality leads to uniform farfield radiation patterns along the azimuth plane (for vertically placed antenna) which gives uniform data transfer rates about the antenna axis.

Printed dipole and monopole antennas are the strongest candidates for planar omnidirectional antennas. They are small in size and compact and therefore can be integrated efficiently with other systems. Various such antennas have been studied in literature.

In [1], authors have demonstrated a triple-frequency antenna for sub-GHz wireless communication, whereas the authors of [2] have presented a triple band antenna for WLAN/WiMAX applications within a short range. For designing a printed dipole, a balanced feed is sometimes necessary to provide improved performance of the antenna. An integrated microstrip balun has been investigated in [3], which follows the theory of a coaxial balun structure proposed in [4], [5]. In [6], the authors have reported a planar tri-band antenna for access points of WLAN/Wi-Fi.

The antenna structure presented in this paper is a printed dipole with such an integrated J-shaped microstrip balun feed. This balun enhances the matching of the structure. Further, two parasitic patches are capacitively coupled to the dipole to bring into prominence the triple band nature and usage of the antenna. The antenna has very good matching at the required frequencies with simulated 10dB bandwidths of 2.2GHz-3.6GHz and 5.2GHz-5.34GHz, thereby finding applications in many of the WLAN bands concerned. The structure is very simple and has the advantage of being planar.

The radiation pattern simulated for the 2.48GHz centre frequency is identical to a dipole antenna. The 3.44GHz and 5.26GHz radiation patterns are oppositely directed and therefore with fast enough switching, both can be used almost simultaneously with high isolation for short range directive communication purposes.

3.2 ANTENNA CONFIGURATION

The antenna structure is designed using CST Studio Suite® and presented in the figure below.

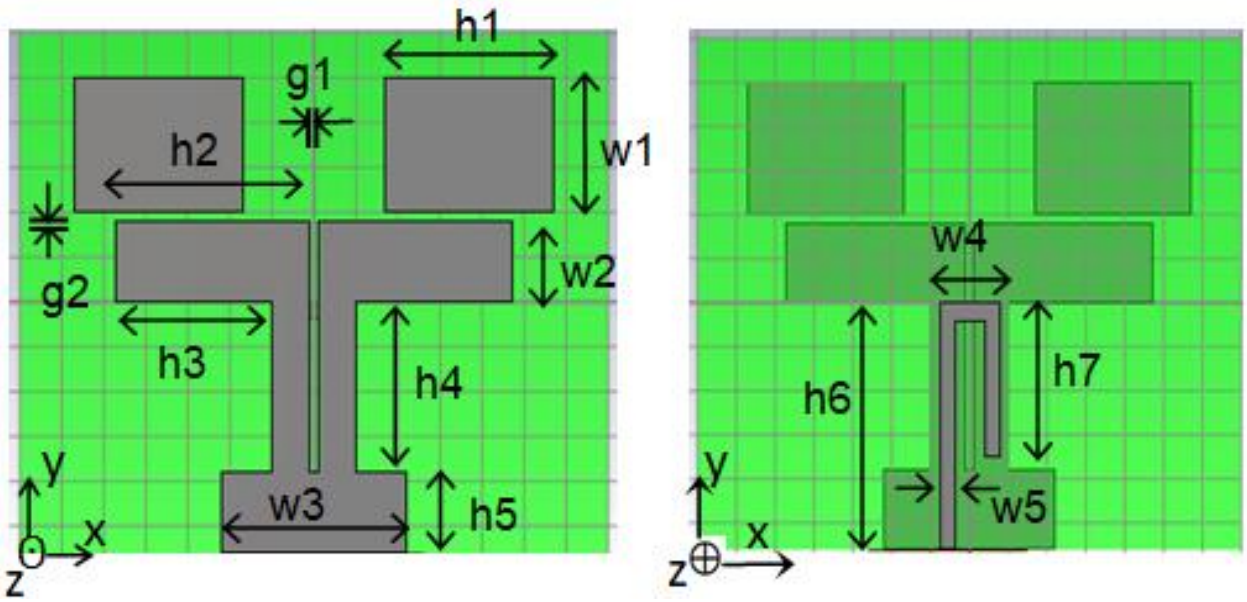

(a) (b)

Fig 3.1. The designed antenna structure with (a) top view and (b) bottom view.

On the top surface, we see the printed dipole structure having arm lengths h2 each fed by coplanar strips of length h4. There is a small ground structure with width w3 and height h5 which acts as the ground plane for the microstrip line on the bottom surface. We see two parasitic patches capacitively coupled to the dipole whose function we shall see later in the chapter.

On the bottom surface is the microstrip feed line which acts as a J-shaped balun and converts the unbalanced microstrip input to a balanced one for the dipole.

The dimensions of the structure are 70x58x1.52 mm^3. It has been designed using PECs (for the antenna structure) with FR-4 as the antenna substrate dielectric. FR-4 has a dielectric constant $\in_r = 4.4$.

The length of the main dipole arms (h2 in figure) are ~ $\lambda_g/4$ each (λ_g = guided wavelength) at 2.45 GHz for the best dipole like radiation pattern.

The dimensions of the structure are shown in the following table below.

TABLE 3.1
DIMENSIONS OF THE STRUCTURE

Name	Dimension(mm)	Name	Dimension(mm)
h1	20	h2	23
h3	18.5	h4	19
h5	9	h6	28
h7	17.5	w1	15
w2	9	w3	22
w4	7.7	w5	2
g1	1	g2	1

All the dimensions have been optimized to result in the most desired performance of the antenna structure.

3.2.1 BALUN CONFIGURATION

Since the dipole antenna is a balanced structure, it needs a balanced transmission line to feed it so that it works efficiently and there is equal current distribution (with opposite phase) in both arms of the dipole. Many such balun structures have been designed and studied in literature. The balun is short for balanced-unbalanced and as the name suggests, it converts a balanced input into an unbalanced one and vice versa.

Baluns are very important for feeding balanced structures with conventional unbalanced feed mechanisms like the microstrip line, slot line, coplanar waveguides or coaxial cables.

In [4] and [5], a coaxial-balun structure has been proposed. The balun structure and its equivalent are shown below.

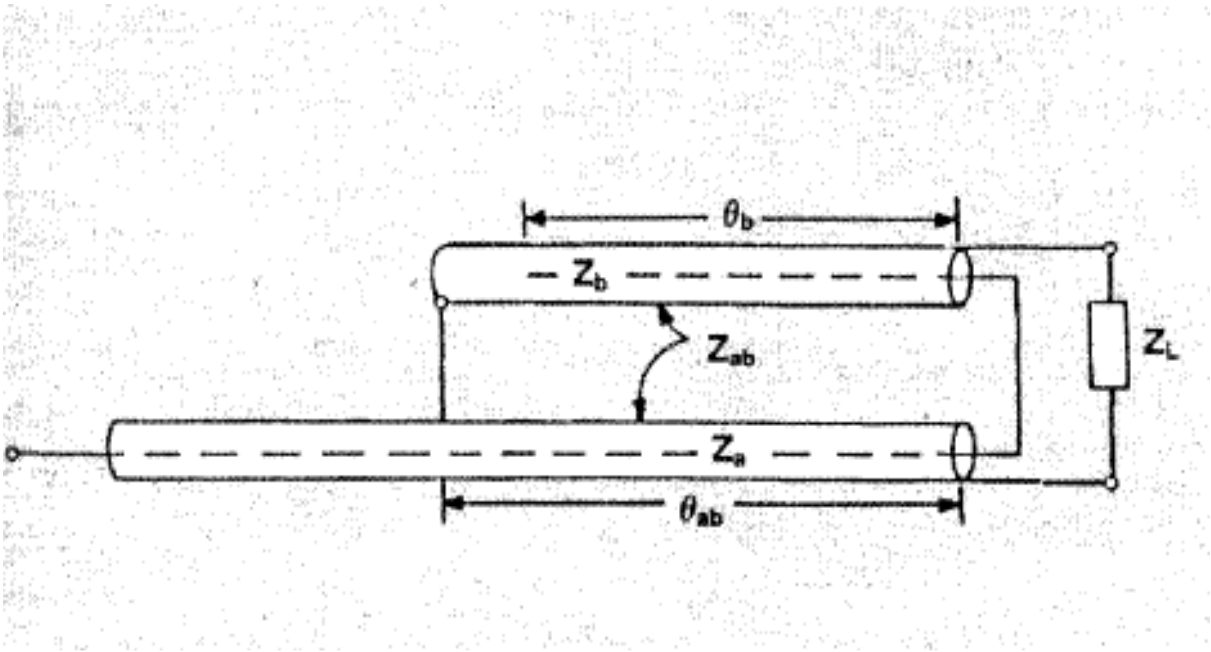

Fig. 3.2. The coaxial-balun structure of [4], [5]. Picture taken from [3].

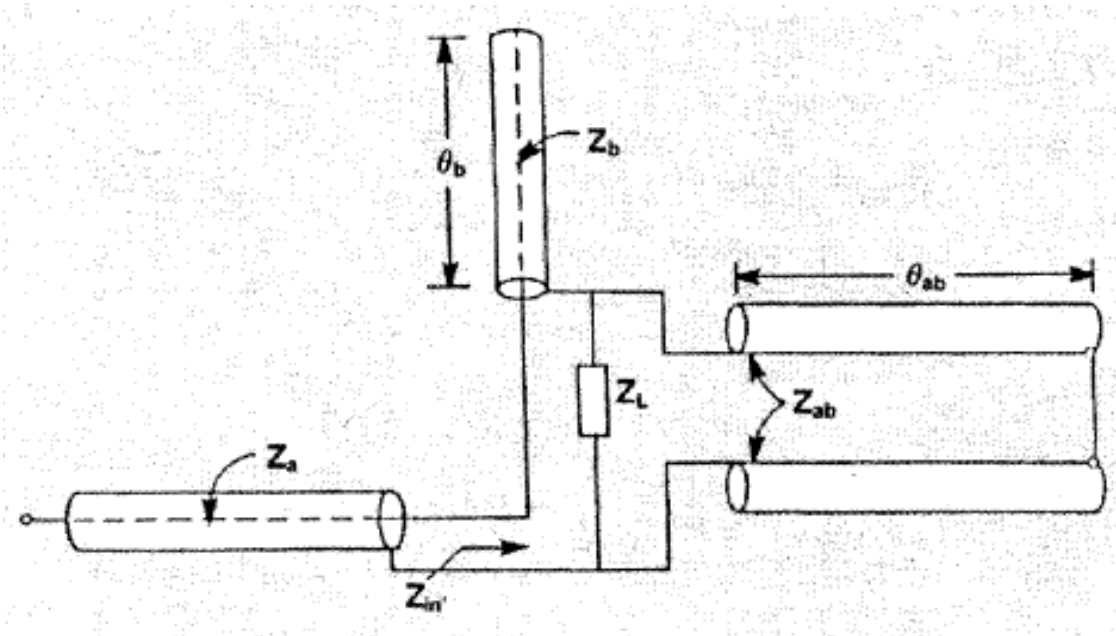

Fig. 3.3. The equivalent structure of the coaxial-balun of [4], [5]. Picture taken from [3].

From the previous figures, it can be seen that the unbalanced input to the balun is given to the left and a balanced output is achieved across the load impedance $Z_{L.}$ Z_L is nothing but the input impedance of the structure we want to feed to the balun (in our case the dipole antenna).

From Fig. 3.3., it can be seen that the balun configuration can be simplified in order to easily achieve an equivalent circuit from where the equivalent input impedance to the balun structure ($Z_{in'}$) can be calculated.

The equivalent input impedance (Z_{in}) seen looking towards the load from the end of the single-ended coaxial line (leftmost in Fig. 3.3) is given by

$$Z_{in'} = -jZ_b \cot\theta_b + \frac{jZ_L Z_{ab} \tan\theta_{ab}}{Z_L + jZ_{ab} \tan\theta_{ab}} \quad . \qquad (1)$$

The first term on the right hand side of equation (1) represents the impedance due to the open-circuit stub (Z_b); the second term is due to the equivalent parallel impedance of the short-circuited coaxial stub (Z_{ab}) in parallel with load $Z_{L.}$

It can be duly noted that $Z_{in'} = Z_L$ when both the stubs are designed to be quarter-wavelengths in dimension, i.e. $\Theta_{ab} = \Theta_b = 90^0$.

Further, the line having impedance Z_a can be used as a quarter-wave transformer to match the equivalent input impedance ($Z_{in'} = Z_L$) to 50Ω. The impedance Z_a can therefore be chosen as

$$Z_a = \sqrt{50 Z_{in'}} \quad . \qquad (2)$$

The dimensions of the line can be optimized further to get much better impedance bandwidth for the structure.

Therefore, this system forms an efficient balun which can be used and adapted for many applications.

The J-shaped microstrip balun used for the antenna in the thesis is based on the above mentioned coaxial-balun structure and theory. It is therefore of great importance to fully understand the working and principle of the coaxial – balun as presented in the current section.

It consists of the three parts as follows:-

1) Quarter-wave microstrip line (characteristic impedance Z_a)

2) Quarter-wave open-circuited stub formed by a microstrip line (characteristic impedance Z_b)

3) Quarter-wave short-circuited stub formed by balanced lines in the form of coplanar strips (characteristic impedance Z_{ab}).

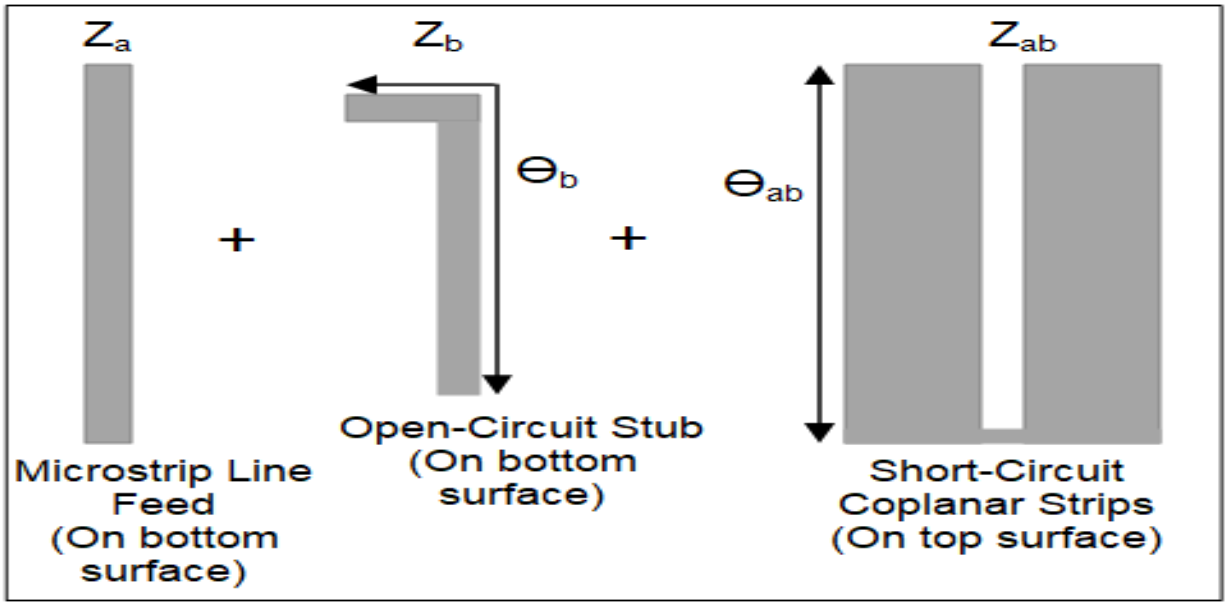

Fig. 3.4. The equivalent parts of the microstrip integrated balun structure used.

The figure above shows the various individual parts which combine to form the microstrip planar balun structure which is used in the design of the antenna in the thesis.

This balun converts the unbalanced microstrip line input to the balanced coplanar strips input which then feeds the designed printed dipole structure.

The lengths and widths of the microstrip line feed, the open circuit microstrip stub and the coplanar strips are all optimized to give the best performance and good impedance bandwidth for operation.

3.2.2 LOADED PARASITIC PATCHES

The addition of the parasitic patches on top of the dipole alters the return loss characteristics and helps in achieving much better matching at the 5.26GHz band. A comparative figure (Fig. 3.5) shows the simulated return loss graph for the structure with and without the parasitic patches. The length and width of the patches have been optimized to give the best return loss characteristics for operation.

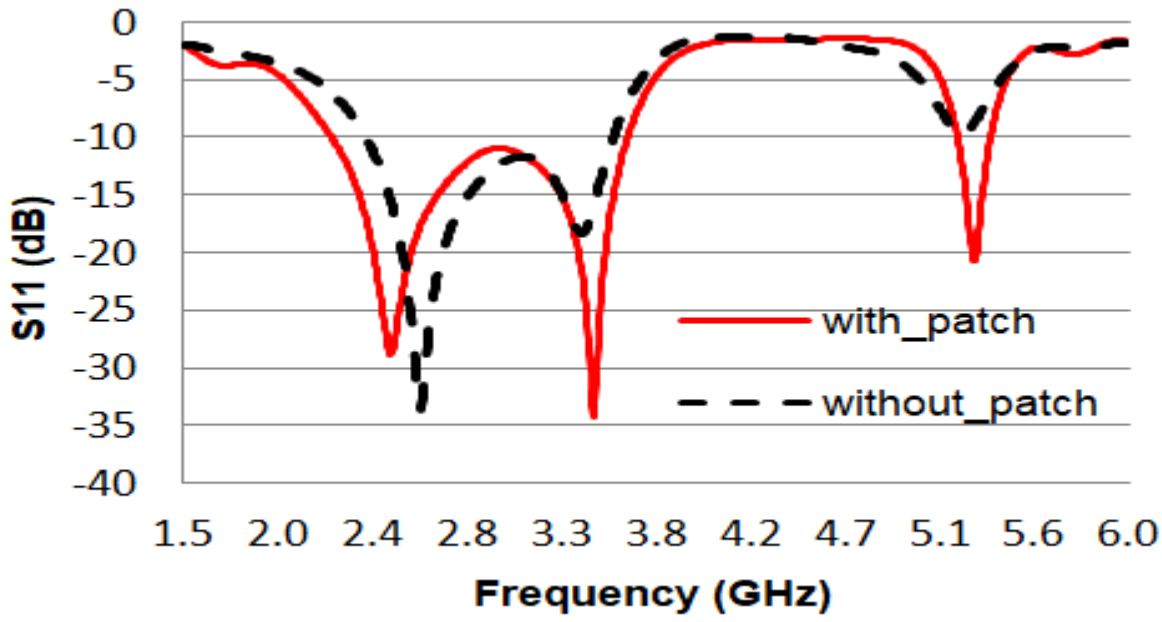

Fig. 3.5. Reflection coefficient plot of the structure with and without the parasitic patches.

As can be seen from the graph, the addition of the capacitive coupled patches enhances matching for both in the 3.44 GHz and 5.26 GHz bands by a significant amount.

The patches modify the total equivalent impedance of the antenna structures near the 3.44 GHz and 5.26 GHz regions and thereby improve the matching. This is due to the fact that some amount of field is coupled capacitively to the patches and hence we get slightly different field distributions near 3.44 GHz and 5.26 GHz as it will be shown in the following sections.

3.3 SIMULATED AND MEASURED PARAMETERS

As stated previously, the antenna was designed and simulated in CST Studio Suite®. The antenna was also fabricated and some of the parameters were measured. The fabricated antenna structure is shown in the figure below.

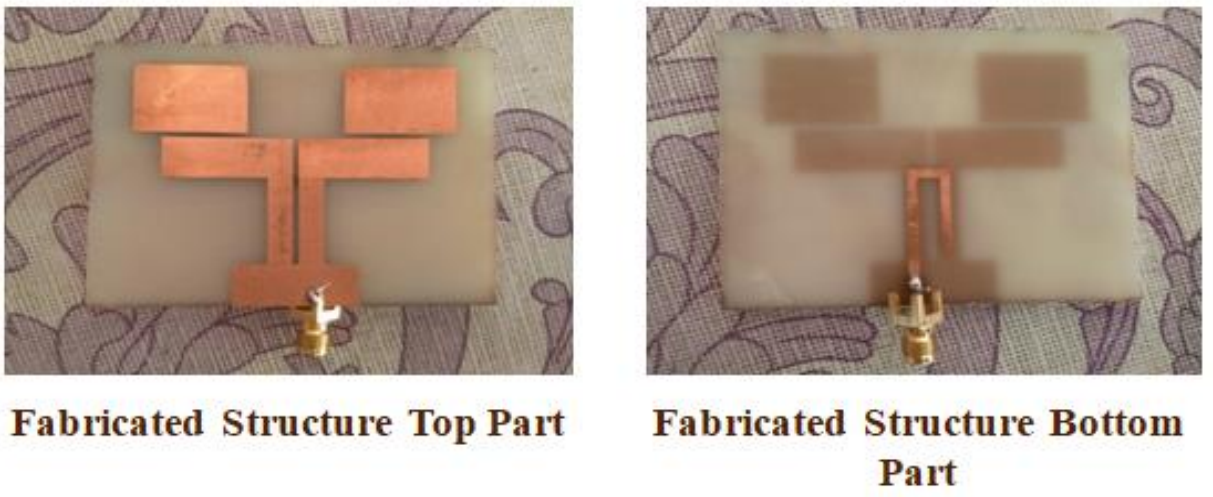

Fig. 3.6. The fabricated antenna structure.

3.3.1 SIMULATED AND MEASURED S11 PLOT

The measured and simulated s11 vs. frequency plots are shown below.

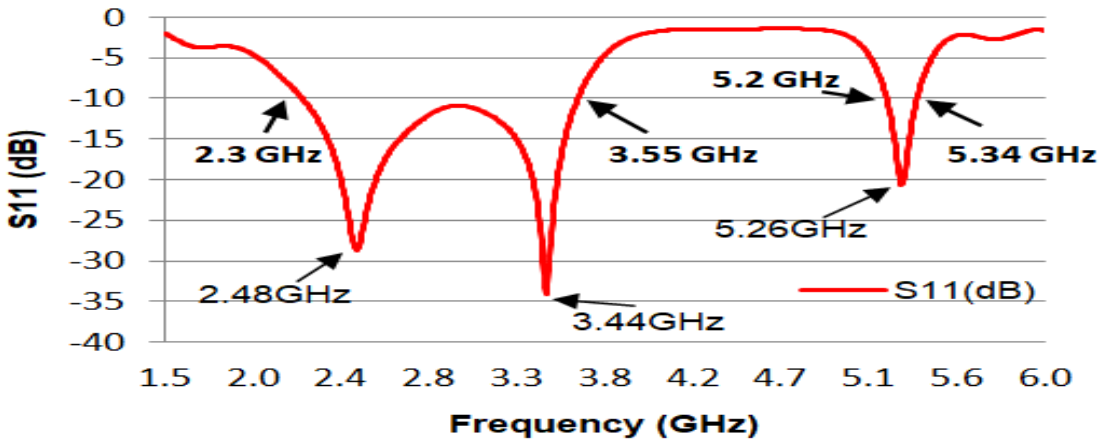

(a)

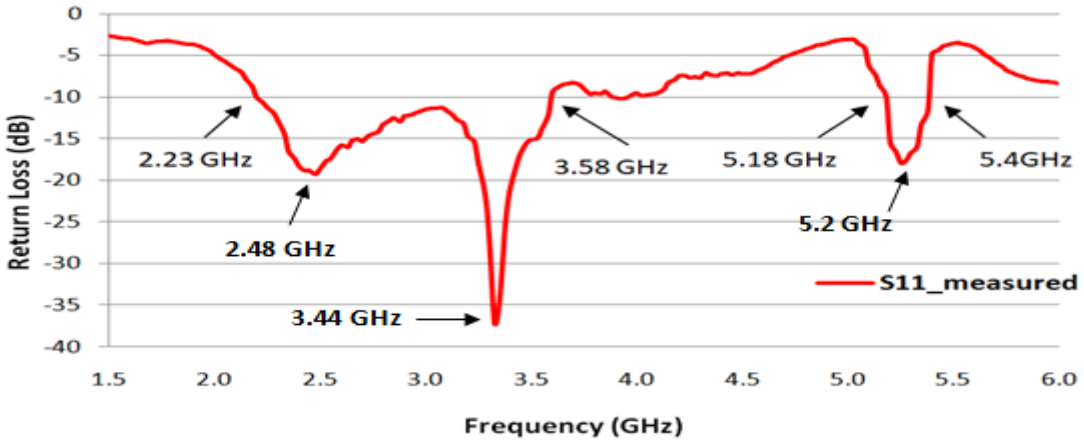

(b)

Fig. 3.7. The S11 parameters of the (a) simulated antenna and (b) fabricated antenna.

It can be seen that the designed antenna shows good triple band resonance capabilities and a wide bandwidth in the 2.2GHz to 3.6GHz region with an added resonance near 5.26GHz due to the addition of the parasitic patches. All these frequencies are very important for wireless communication purposes. The simulated s11 and measured s11 are very similar in nature. From the measured s11, a -10dB bandwidth of (3.58GHz-2.23GHz) 1.35 GHz and (5.4GHz-5.18GHz) 220MHz is achieved. Therefore the antenna resonates properly in the required WLAN (2.5GHz, 5.2GHz) regions and the WiMAX (3.5 GHz) region. The designed antenna is also wideband in nature.

It is seen therefore that the antenna accepts most of the input power at the required frequencies with very little reflection. However, whether the antenna can act as an efficient radiator or not can only be known from the radiation efficiency of the antenna at the desired frequencies. VNA model E5071B (300 kHz-8.5GHz) from Agilent Technologies was used to measure s11.

3.3.2 SIMULATED SURFACE CURRENT DISTRIBUTIONS

The surface current distribution at the desired frequencies speak a great deal about how well the antenna can radiate and which parts of the antenna radiate at which particular frequency. It also gives an idea about where the nulls and peaks of the radiation pattern will form. The simulated surface current distributions are given in the next page.

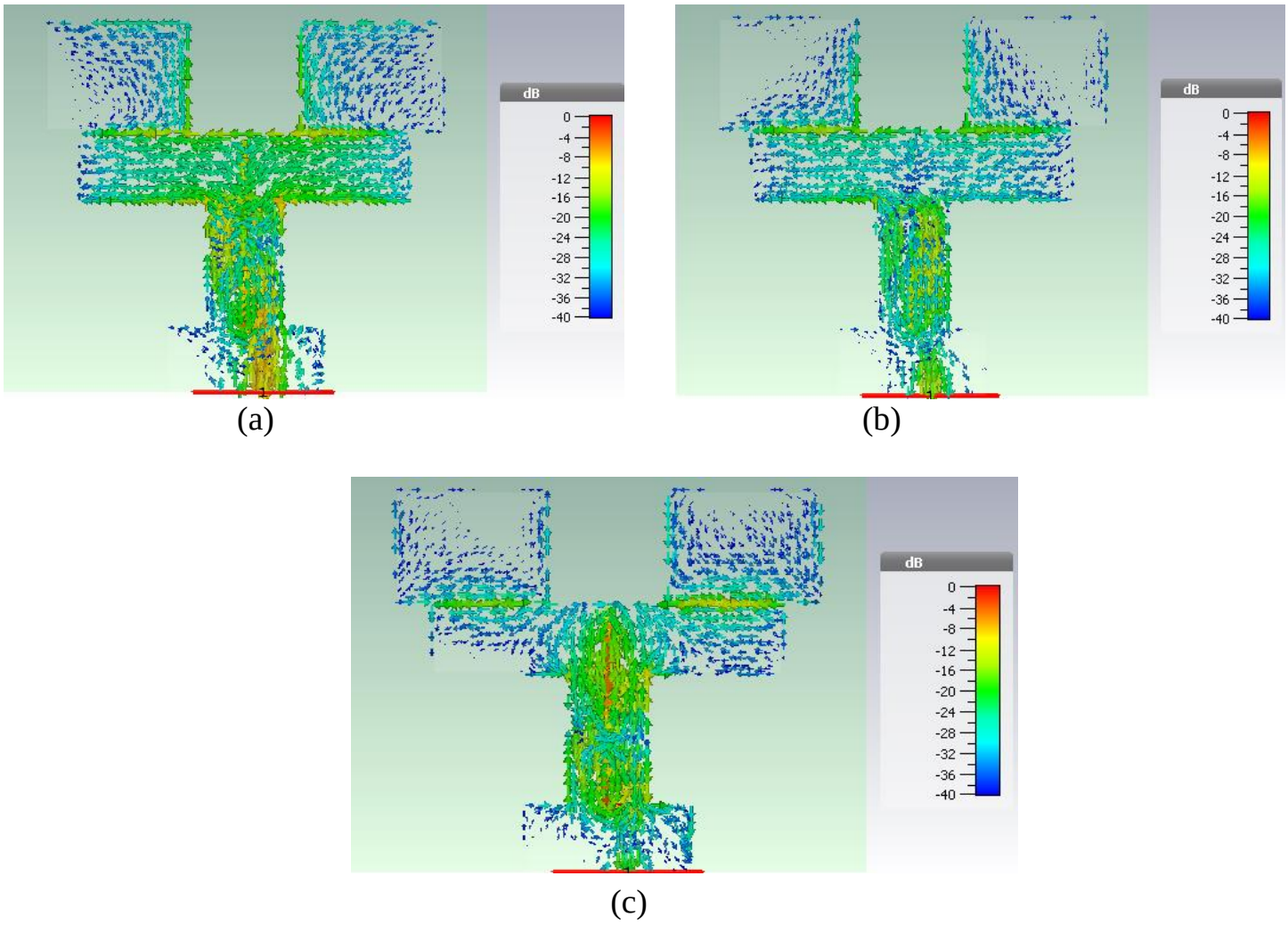

Fig 3.8. Simulated surface current distributions at (a) 2.45 GHz, (b) 3.5 GHz and (c) 5.2 GHz.

It can be seen that the surface currents for the 2.45GHz and 3.5 GHz regions are similar. The surface currents along the dipole are somewhat similar to those for normal wire dipoles. There is some amount of coupling between the patches and the dipole as was already discussed previously. For the 5.2 GHz region, it can be seen the current distribution is a little different from a normal dipole and therefore the radiation pattern must diverge from the general omnidirectional dipole radiation pattern as it will be shown in the following section.

In all the three cases, there is only moderate coupling of fields between the dipole and the patches which does not hamper the radiation patterns of the antenna structure to a large degree.

3.3.3 SIMULATED AND MEASURED FAR FIELD RADIATION PATTERNS

The farfield radiation pattern polar plots have been given below. Both the simulated and measured radiation patterns are presented in the same plot for the two planes xz and yz. Transmitter antenna used was 800MHz-18GHz Double Ridged Broadband Horn Antenna (Model HA-08M18G-NF).

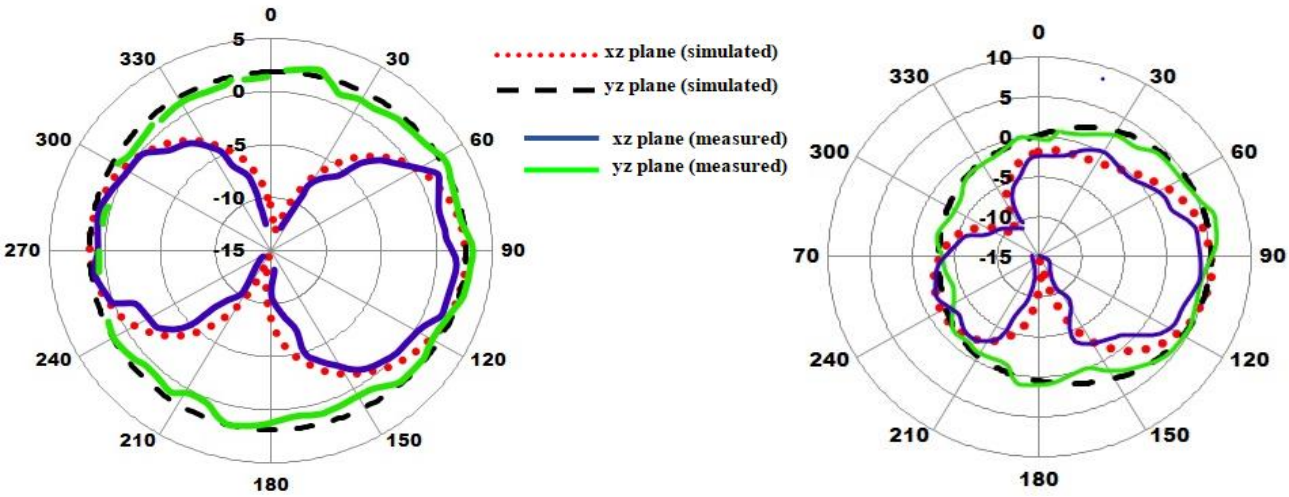

(a) (b)

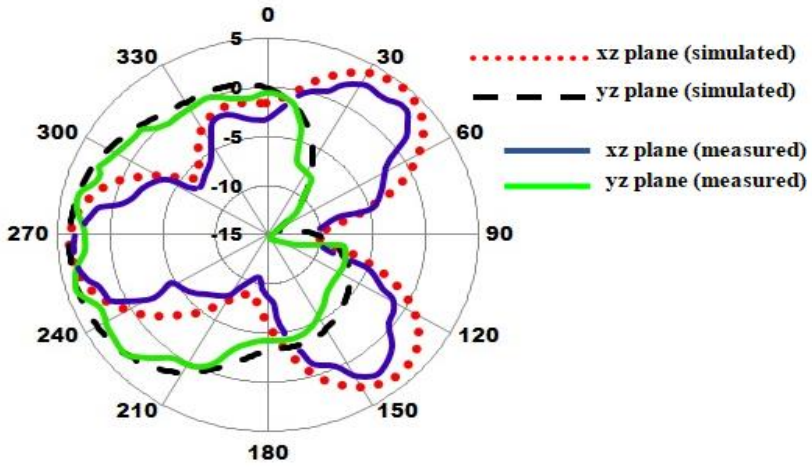

(c)

Fig. 3.9. Farfield radiation patterns for (a) 2.45GHz, (b) 3.5 GHz and (c) 5.2 GHz.

It is observed that the radiation pattern at 2.45GHz almost perfectly resembles a simple dipole antenna radiation pattern. Therefore, near this frequency, the antenna can be used as a linearly polarized omnidirectional radiator similar to a dipole.

For the second centre frequency of 3.5GHz, the antenna begins showing directional properties. Therefore, the antenna can be used as a directional radiator for communication in this part of the frequency spectrum.

For the third centre frequency of 5.2GHz, the antenna again shows directive properties with the main beam in the xz plane having three distinct lobes. The antenna can again be used as a directional radiator, this time also in a direction opposite to the previous case. Therefore, the antenna has the added advantage of carrying out communication at two different frequencies in different directions with high isolation almost simultaneously with fast enough switching equipment.

3.3.4 RADIATION EFFICIENCY AND GAIN

The radiation efficiency determines whether the antenna can radiate efficiently in the frequencies of interest. The simulated radiation efficiency vs. frequency plot is shown below.

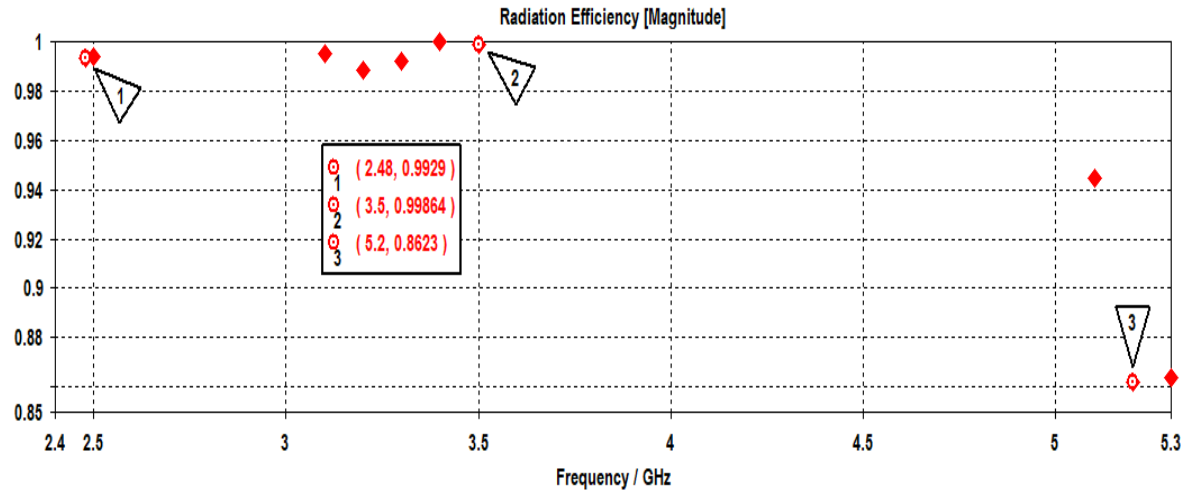

Fig. 3.10. Radiation efficiency vs. frequency as per simulation results.

Therefore it is clear that the antenna is an efficient radiator at the frequencies of interest with radiation efficiencies of 0.99, 0.99 and 0.86 at 2.48GHz, 3.5 GHz

and 5.2 GHz respectively. The following table gives the gain and radiation efficiency of the designed antenna.

TABLE 3.2

SIMULATED PARAMETERS AT FREQUENCIES OF OPERATION

Frequency(GHz)	Gain(dBi)	Radiation Efficiency (Magnitude)
2.45	**2.65**	**0.99**
3.5	**5.41**	**0.99**
5.2	**4.14**	**0.87**

Therefore it can be seen that at 2.45 GHz, the gain is similar to that of a dipole while at the other two frequencies the gain has increased due to increase in directionality of the pattern as discussed previously.

3.4 CONCLUSION

The proposed antenna is very simple to design and fabricate and has the advantage of being planar. The designed antenna shows good triple band resonance capabilities and a wide bandwidth in the 2.2GHz to 3.6GHz region with an added efficient resonance near 5.26GHz due to addition of the parasitic patches. The balanced feed ensures better operation of the structure as well as matching the antenna structure to the usual 50Ω port systems found in most cases.

The IEEE Standards which are compatible with this structure include IEEE 802.11b/g/n (WLAN, 2.4GHz region) and IEEE 802.16d (WiMAX, 3.5GHz region). For the 5.2GHz region, some of the IEEE 802.11a/h/j/n/ac/ax standards (WLAN) can be used depending upon which of these fall within the 10dB bandwidth of the antenna for the 5.26GHz resonance region. The IEEE 802.16e standard (WiMAX, 2.3GHz, 2.5GHz and 3.5GHz) can be used as well. The channel bandwidths for each of the above standards are also covered by the proposed structure.

REFERENCES

[1] S. Genovesi, A. Monorchio and S. Saponara, “Compact triple-frequency antenna for sub-GHz wireless communications,” IEEE Antennas and Wireless Propagation Letters, Vol. 11, pp. 14-17, 2012

[2] K. George Thomas and M. Sreenivasan, “A novel triple band printed antenna for WLAN/WiMAX applications,” Microwave and Optical Technology Letters, Vol. 51, No. 10, pp. 2481-2485, October 2009

[3] D. Edward and D. Rees, "A broadband printed dipole with integrated balun," Microwave Journal, pp. 339-344, May 1987.

[4] W. K. Roberts, "A new wide band balun," Proceedings of the IRE, vol. 45, pp. 1628-1631, Dec. 1957.

[5] G. Oltman, "The compensated balun," IEEE Trans. Microwave Theory Tech., Vol. 14, pp. 1628-1631, Mar. 1966.

[6] R.L. Li, X.L. Quan, Y.H. Cui and M.M. Tentzeris, “Directional triple-band planar antenna for WLAN/WiMax access points,” Electronics Letters., pp. 305-306, 15th March 2012 Vol. 48 No. 6

CHAPTER - IV

EFFECTS OF TWO DIFFERENT MODIFIED GROUND PLANES ON AN EQUILATERAL TRIANGULAR RING SHAPED PATCH ANTENNA

4.1 INTRODUCTION

Triangular patch antennas have been studied theoretically and experimentally as an alternative to rectangular patch antennas. Triangular patch antennas are most of the times smaller than the corresponding rectangular patch antennas. Equilateral triangular patch antennas can also support circular polarization given the structures are fed adequately to excite the orthogonal modes.

Triangular ring shaped patch antennas are modified versions of the simple triangular patch and have also been studied in literature. Triangular ring antennas for dual frequency and dual/circular polarizations have been designed and studied in [1]. Simple triangular rings have also been presented in [2], [3]. A similar structure consisting of triangular ring antennas for dual-frequency dual polarization or circular polarization operations is also presented in [4].

However, all the above references have full ground planes and none have studied the effects of modified ground planes on triangular ring antennas. Patch antennas are usually designed with full ground planes to get the distinct directional radiation pattern and moderate gain.

This thesis presents a study by introducing two different modified ground structures and observing their effects on an equilateral triangular ring patch antenna. The purpose of this study is to design antennas where both the metallic patch and the metallic ground plane take part in radiation together as an efficient unit.

Both antennas are designed and fabricated and the simulated and measured data are presented. The designed antenna dimensions are such that the antennas function in the WLAN and/or the WiMAX frequency regions.

It will be seen that in both cases, the ground planes also take part in radiation and in both cases modify the resonance frequency of the structures significantly. The antennas are low profile, planar and wideband in nature, thereby making them good candidates as antennas for portable wireless communication devices. The sizes of the antennas are also pretty small with both the antennas having an area of 40x40 mm^2.

4.2 ANTENNA STRUCTURES

The proposed antennas with the modified ground planes have been designed and simulated using CST Studio Suite® and fabricated for experimental verification. The designed and fabricated structures are shown in the figures below.

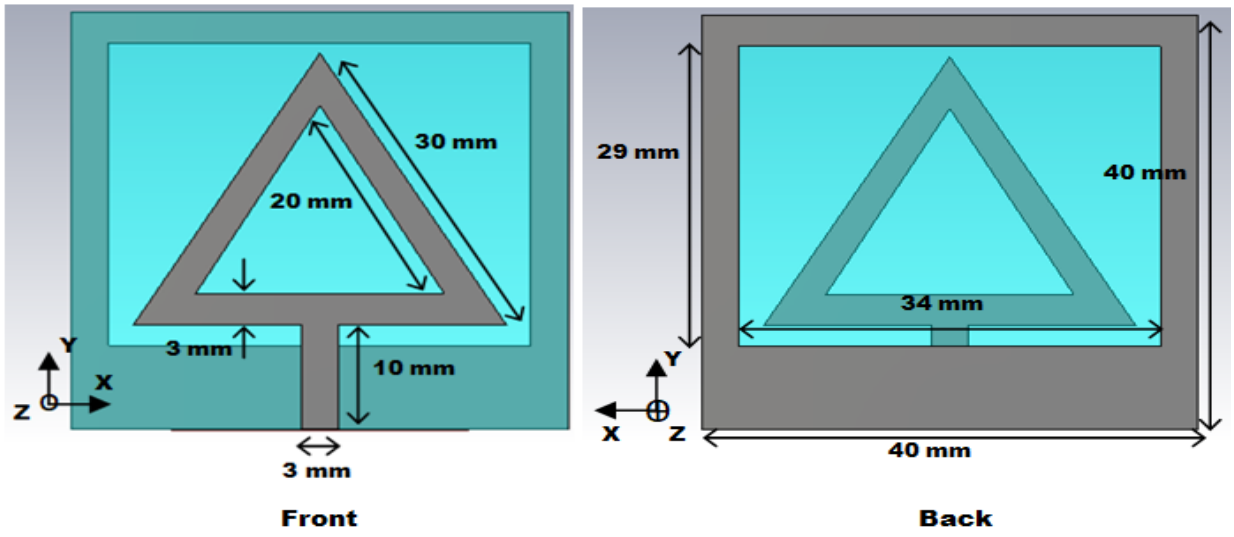

(a)

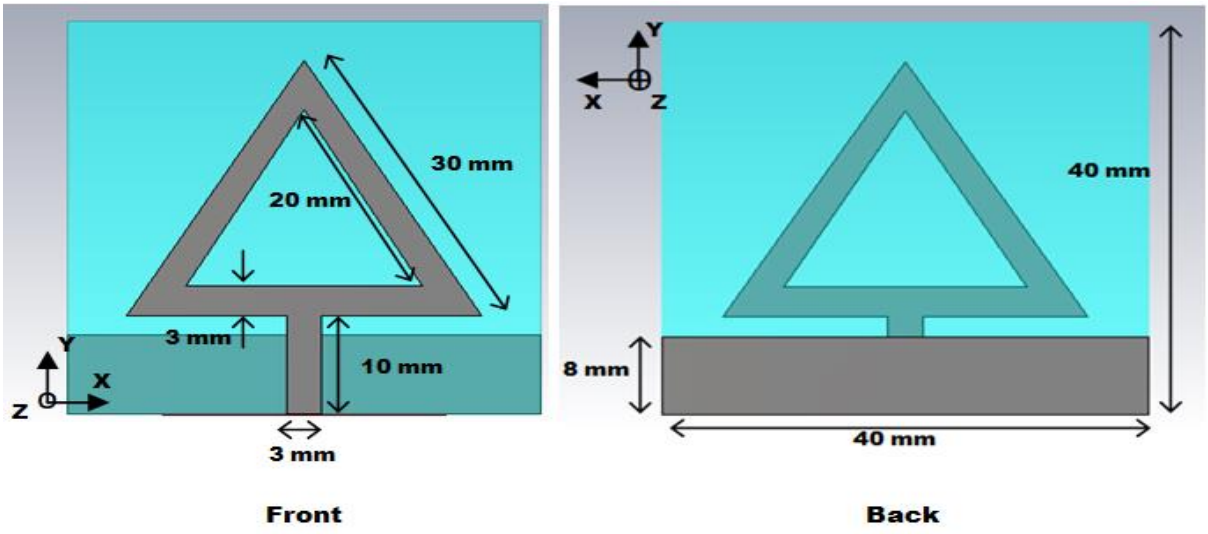

(b)

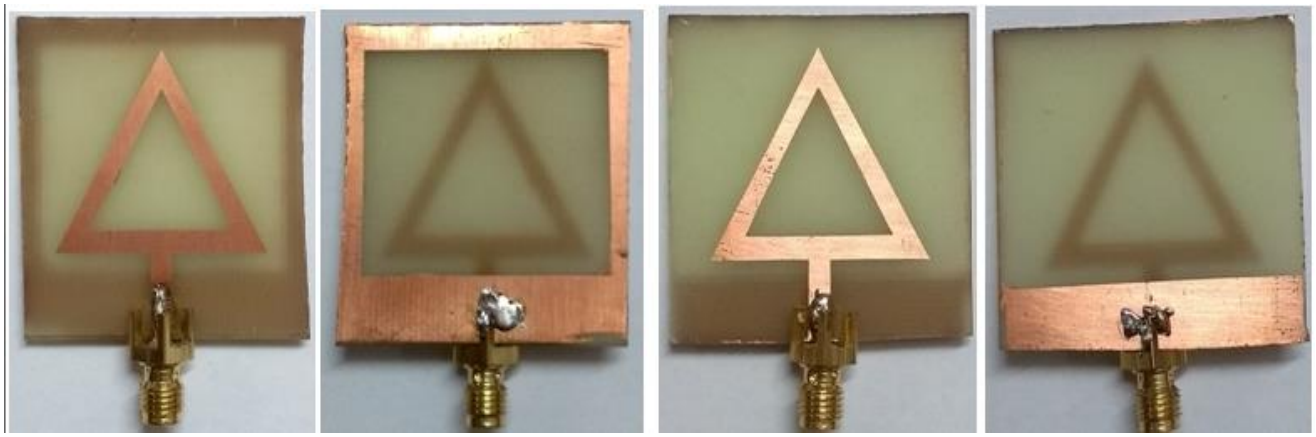

Front Back Front Back

Window defect **Simple defect**

(c)

Fig. 4.1. The equilateral triangular ring antennas with (a) window defect ground plane, (b) simple defect ground plane and (c) the two fabricated structures.

The two designed and fabricated structures are of identical size (40 x 40 x 1.52 mm^3). FR-4 is used as the substrate for both structures with dielectric constant $\varepsilon_r = 4.4$ and loss tangent $\tan\delta = 0.02$.

The dimensions of the equilateral triangular ring shaped patch are chosen such that the mean perimeter of the rings is approximately a wavelength (free space wavelength) long at around 4 GHz. The addition of the modified ground planes affect the characteristics of the antenna and also the radiation patterns as will be seen in the following sections.

Two different ground planes are selected and studied. The first one, Fig. 4.1 (a), consists of a ground plane with the central part (window) etched out and therefore named the window defect. The second one, Fig. 4.1 (b), consists of a simple defected ground plane normally used for ultrawideband antenna structures.

The fabricated structures are also presented in Fig. 4.1 (c) with both front and back view properly labelled. The antennas are quite small in size.

4.3 SIMULATED AND MEASURED ANTENNA PARAMETERS

The simulated and measured antenna parameters are presented in this section and it will be seen that the measured and simulated antenna parameters are in good agreement with one another.

4.3.1 SIMULATED AND MEASURED REFLECTION COEFFICIENTS

The analyzed frequency range of both the structures is set from 1 GHz to 6 GHz. The simulated and measured s11 are shown in Fig. 4.2. The measured and simulated s11 plots of both the antennas are provided in a single graph for better understanding and comparison purposes. The simulated and measured results are in good agreement. VNA model E5071B (300 kHz-8.5GHz) from Agilent Technologies was used to measure s11.

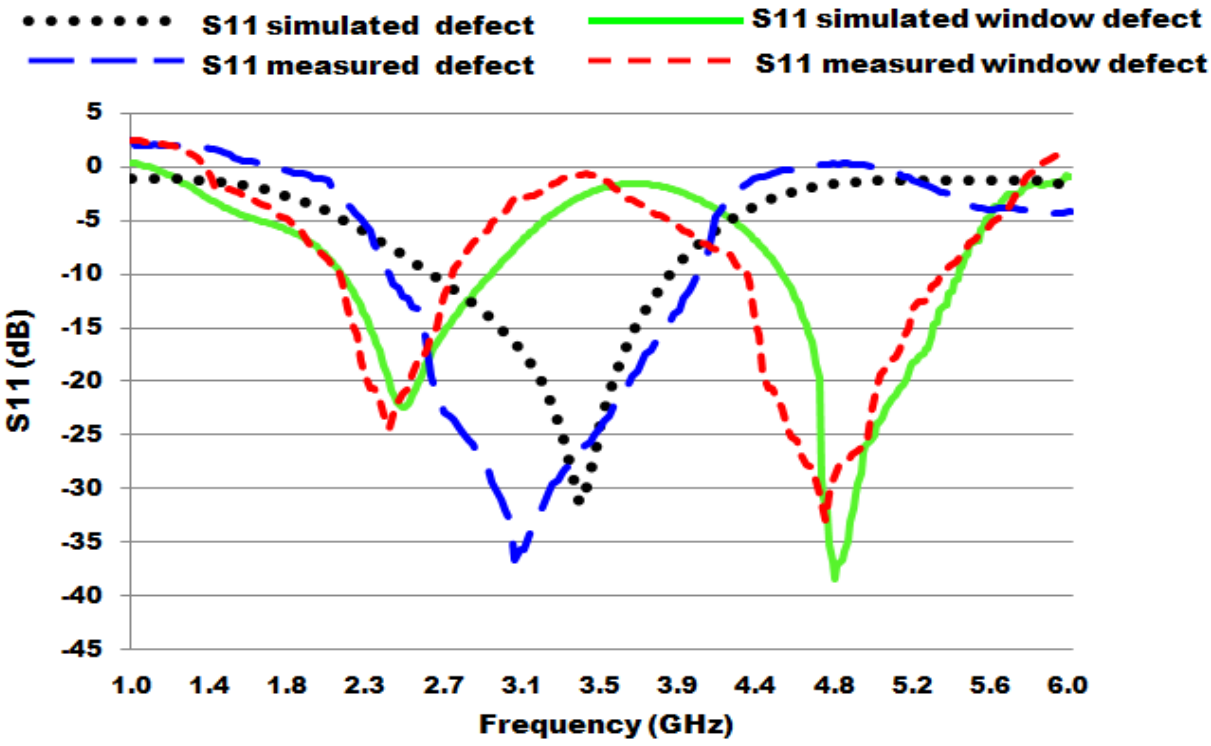

Fig. 4.2 Simulated and measured s11 of the two antenna structures.

It is seen that the antenna with window defect (Fig. 4.1 (a)) has two bands of operation. The 10dB bandwidth is measured from 2.1 GHz to 3.1 GHz (1 GHz bandwidth) and from 4.4 GHz to 5.3 GHz (900 MHz bandwidth), resulting in percentage bandwidths of 38.5% and 18.5% respectively. Therefore it covers the 2.4/5.2 GHz WLAN bands.

The antenna with simple defect (Fig. 4.1 (b)) has a single band of operation. The 10dB bandwidth is measured from 2.65GHz to 3.9 GHz (1.25 GHz bandwidth), resulting in a percentage bandwidth of 38%. It therefore covers the 3.5 GHz WiMAX band.

The designed antennas are thus found to be wideband in nature with good matching at the frequencies of interest. They are also found to cover the popular IEEE standard communication channels as seen from Fig. 4.2.

Low values of s11 ensure that the input power is accepted by the antenna structures with very little reflection at the input terminals. However, to find out whether the antennas can act as efficient radiators in the regions of good s11, the radiation efficiency of the antenna structures needs to be studied at the required frequencies. This is shown in the following sections as well.

4.3.2 SIMULATED SURFACE CURRENT DISTRIBUTIONS

The surface current distribution at the desired frequencies speak a great deal about how well the antenna can radiate and which parts of the antenna radiate at which particular frequency. It also gives an idea about where the nulls and peaks of the radiation pattern will form. The simulated surface current distributions are given in the following figures.

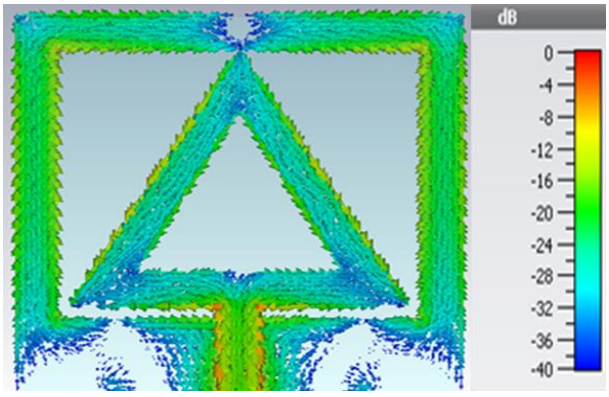

(a)

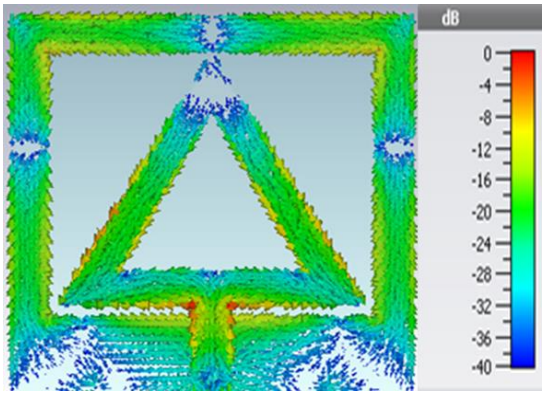

(b)

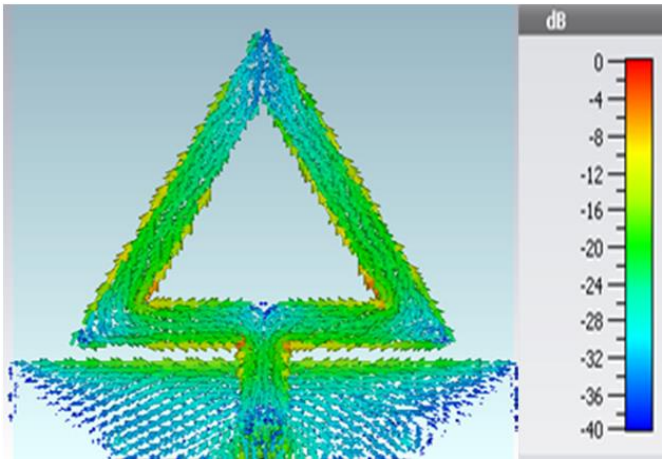

(c)

Fig. 4.3. Simulated current distributions for (a) window defect at 2.45GHz, (b) window defect at 5.2 GHz and (c) simple defect at 3.5 GHz.

It is seen that in all three cases, especially in the antenna with window defect, there is significant surface current present on the ground planes as well. This confirms the fact that the ground planes play a big part in determining the resonance frequencies of the structures and subsequently in radiation.

Moreover, for the window defect, a difference between the surface current distribution at 2.45 GHz and at 5.2 GHz can be noticed. More current nulls can be found at the 5.2 GHz from which it can be concluded that the radiation pattern at 5.2 GHz will have more lobes and nulls than the 2.45 GHz frequency.

For the antenna with simple defect ground plane, the current distribution on the triangular ring is found to be similar to that on the triangular ring with window defect at 2.45 GHz. Therefore, they are expected to have similar far field radiation patterns as well.

Therefore a lot about how the antennas operate and radiate can be understood and learnt by studying the surface current distributions. It will also be seen how putting cutting out the ground plane increases the bandwidth of both the antennas and gives a more omnidirectional radiation pattern.

4.3.3 SIMULATED AND MEASURED FARFIELD RADIATION PATTERN

The simulated and measured radiation patterns are shown in Fig. 4.4. Transmitter antenna used was 800MHz-18GHz Double Ridged Broadband Horn Antenna (Model HA-08M18G-NF).

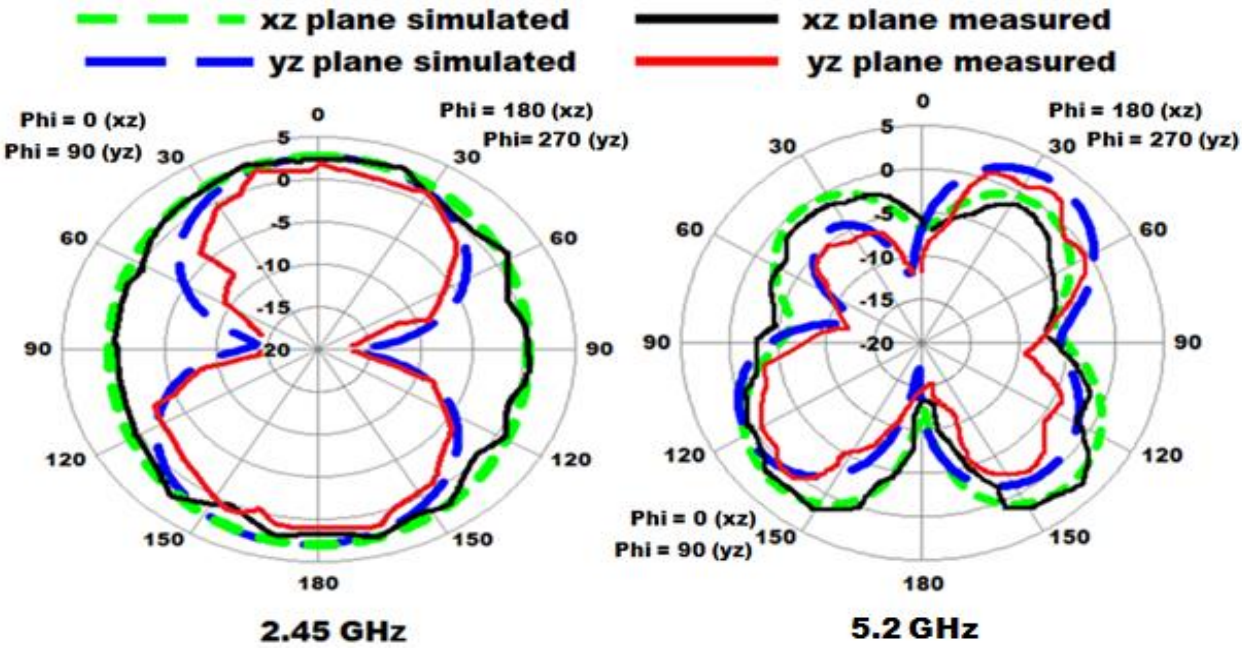

(a)

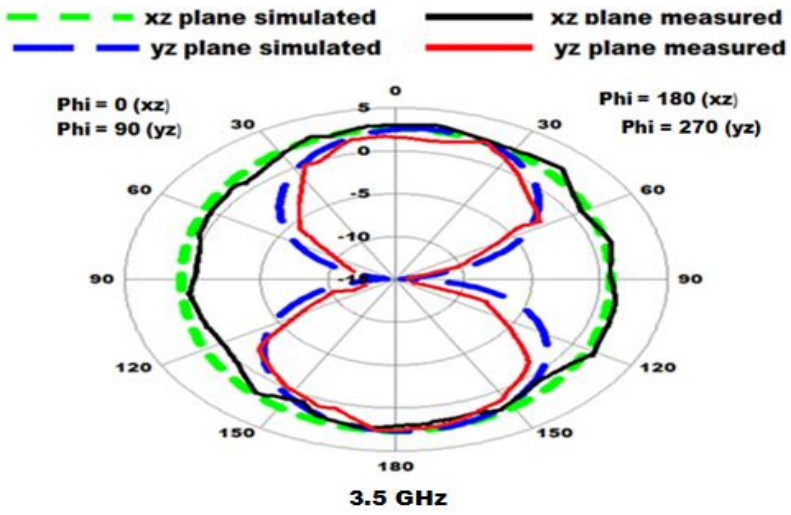

(b)

Fig. 4.4. Simulated and measured radiation patterns for the (a) window defect antenna and (b) simple defect antenna.

It is observed that the antennas are omnidirectional at 2.45GHz and 3.5GHz but slightly directional at 5.2 GHz. Thus, it matches with the conclusions that were drawn from the study of the surface current distributions. The measured cross polarization levels were also pretty low for both the structures in both the xz and yz planes for 2.45GHz, 5.2 GHz (for the window defect antenna) as well as 3.5 GHz (for the simple defect antenna).

4.3.4 RADIATION EFFICIENCY AND GAIN

The simulated radiation efficiency of the antennas vs. frequency is shown below.

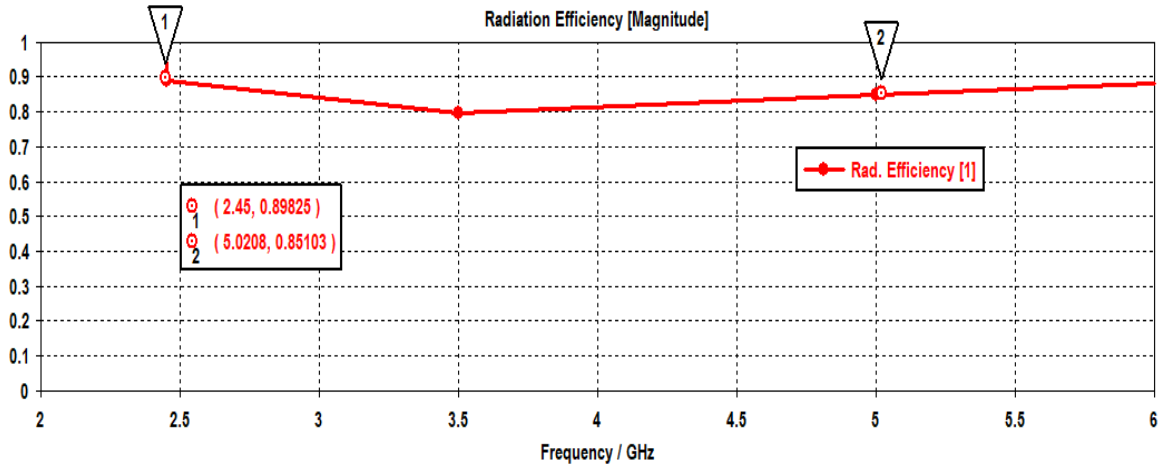

(a)

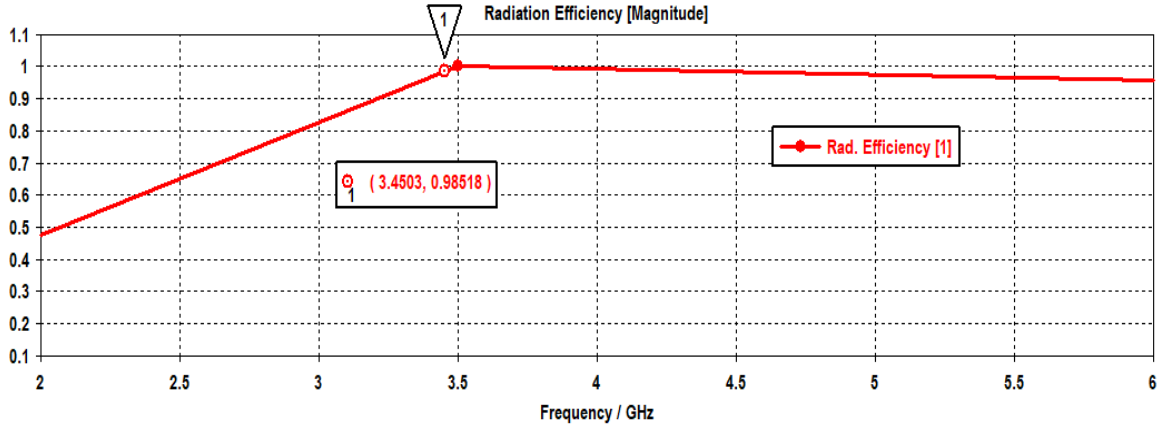

(b)

Fig. 4.5. Simulated radiation efficiency for the (a) window defect antenna and (b) simple defect antenna.

From the above plots it is evident that the antennas are efficient radiators in the respective frequencies of interest.

The maximum gain of the window defect antenna was found to be 2.65 dBi at 2.45 GHz and 3.01 dBi at 5.2 GHz. For the simple defect antenna, the gain was found to be 2.76 dBi near the 3.5 GHz region. Therefore at 2.45 GHz and 3.5 GHz, the antenna behaves almost similar to that of a normal dipole.

4.4 CONCLUSION

Effects of the modified ground planes on the equilateral triangular ring shaped antenna have been studied and presented along with measured results. The antennas have been found to be wideband in nature, linearly polarized, omnidirectional and capable of covering some standard IEEE wireless communication channels with good efficiency.

The antennas are efficient radiators in the frequencies of interest and the effects of the modified ground planes can be noticed from the surface current distributions. It can thus be concluded that the triangular ring shaped patch and the ground planes together radiate as an efficient unit.

REFERENCES

[1] Jin-Sen Chen, "Studies of CPW-fed equilateral triangular-ring slot antennas and triangular-ring slot coupled patch antennas," IEEE transactions on Antennas and Propagation, Vol. 53, No. 7, July 2005, pp. 2208-2211.

[2] Linli Jiang ,Chunlan Lu ,Wenquan Cao ,Changsong Wu ,Feng Yuan, "A dual-band and dual polarized antenna with two nested triangular rings," 2017 Sixth Asia-Pacific Conference on Antennas and Propagation (APCAP), 2017, pp. 1-3.

[3] Tao Zhang, Wei Hong, Ke Wu, "A low-profile triple-band triple-polarization antenna with two triangular rings," IEEE transactions on Antennas and Propagation, Vol.14,2015, pp. 378-381.

[4] Tao Zhang, Yan Zhang,Wei Hong, and KeWu,"Triangular Ring Antennas for Dual-Frequency Dual-Polarization or Circular-Polarization Operations," IEEE Antennas and Wireless Propagation Letters, VOL. 13, 2014, pp. 971-974.

CHAPTER - V

A STAR SHAPED WIDEBAND PATCH ANTENNA WITH CENTRAL CIRCULAR SLOT FOR WLAN AND WIMAX APPLICATIONS

5.1 INTRODUCTION

As stated earlier in this thesis, printed antennas have the advantage of being planar and can be integrated into portable devices such as mobiles for efficient use. Many such printed antennas have been studied in literature. A dual band printed folded dipole antenna is presented in [1] for 2.45 GHz and 3.5 GHz applications. However, the antenna is large in size and also directional at 3.5 GHz. A printed broadband monopole antenna for WLAN/WiMAX is presented in [2]. But the antenna is again large in size, has low gain and very low efficiency. A dual band antenna is presented in [3] but it has numerous parameters which need optimization and careful designing. Many of the antennas in literature are either too complicated to design and optimize, or are large in size, or not omnidirectional in all the operating frequencies.

Therefore, a printed antenna with small size, simple design and more or less omnidirectional pattern throughout the whole band of operation is considered for design in this chapter.

Wideband antennas can be designed by removing part or most of the ground plane of a microstrip patch antenna to allow for more permissible radiation modes to occur naturally as well as to provide an omnidirectional radiation pattern for the structure. Proper impedance matching of such structures leads to very wideband antennas which are omnidirectional throughout most of the -10dB reflection coefficient bandwidth [4].

The antenna presented in this chapter is very wideband, has linear polarization, is small in size, simple and has low cross polarization levels. The overall dimensions of the antenna are 40x40x1.52 mm^3. It is very simple to design and low profile.

The antenna structure has been fabricated and it shall be seen that there is good correspondence between the measured and simulated results. The star shaped antenna also has a central circular slot present which helps in better matching at the operating frequencies without much affecting the other parameters. The details of the designed antenna and the various parameters are presented in the following sections.

5.2 ANTENNA STRUCTURE

The antenna has been designed and simulated using CST Studio Suite®. It has also been fabricated. The designed and fabricated structures are shown in the following figures.

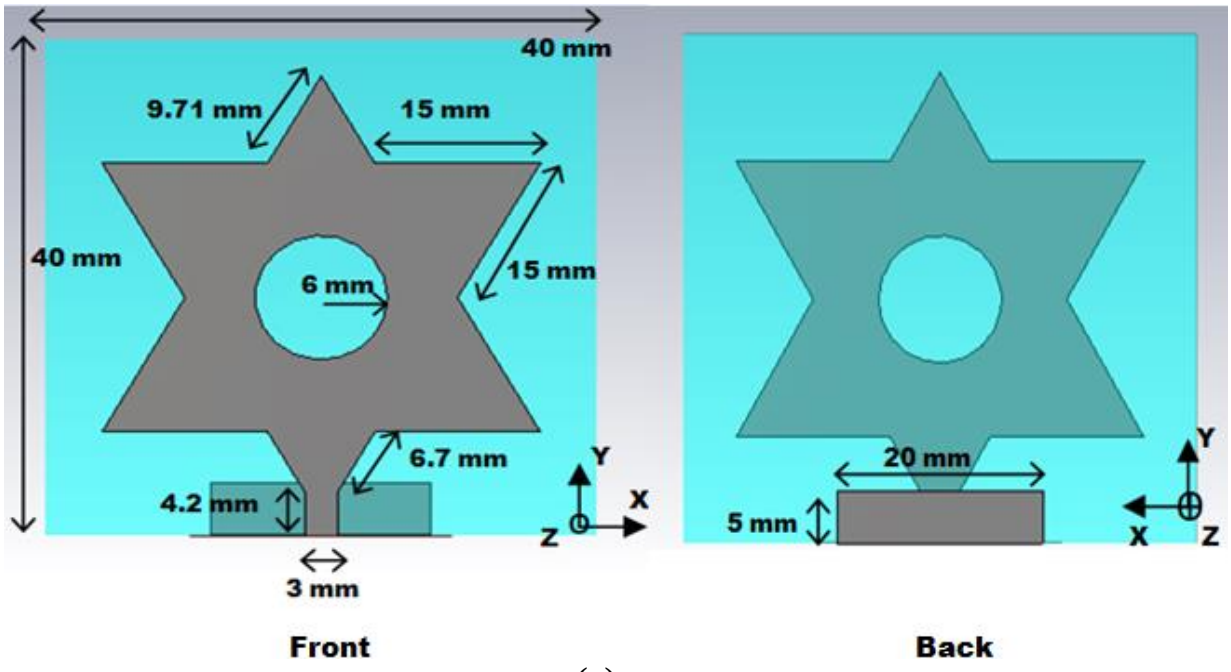

(a)

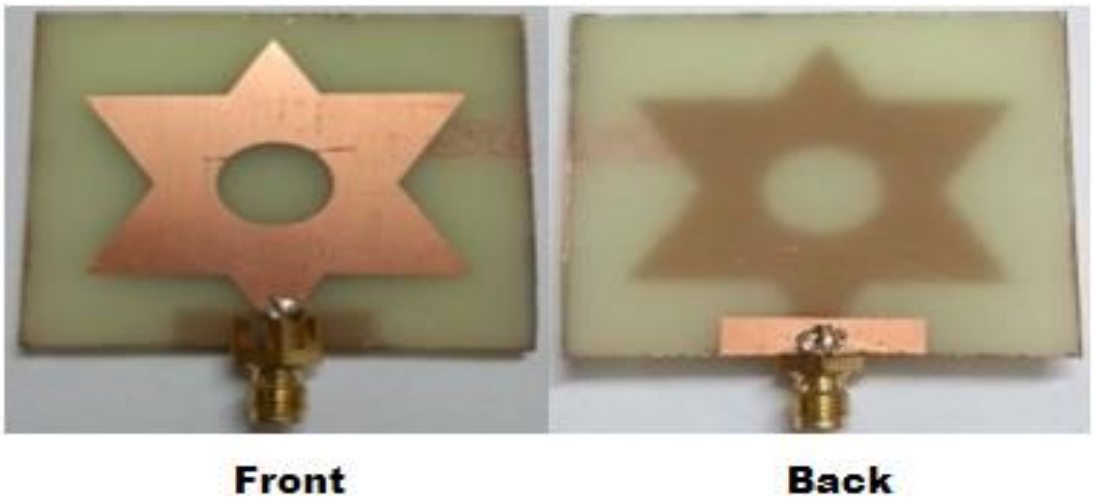

(b)

Fig 5.1. (a) Simulated antenna structure and (b) the fabricated product.

The dimensions of the antenna are 40x40x1.52 mm^3. The antenna is designed and fabricated on FR-4 substrate with $\varepsilon_r = 4.4$ and $\tan\delta = 0.02$.

The star shaped antenna is made by initially taking an equilateral triangular patch antenna of length 30mm and hence a perimeter of 90mm. A copy of the triangular patch is then made, inverted and translated until both the triangles have the same centroid. The various dimensions of the ground planes are studied via a parametric sweep and the best ground dimensions are chosen which gives the largest bandwidth, as will be shown in the sections below. It will also be shown that the addition of the central slot leads to better matching at the frequencies of interest.

5.2.1 ADDITION OF CENTRAL CIRCULAR SLOT

Keeping all the other dimensions same, the star shaped antenna s11 parameters are studied with and without the central circular slot. The comparison done in simulation is shown in the figure below.

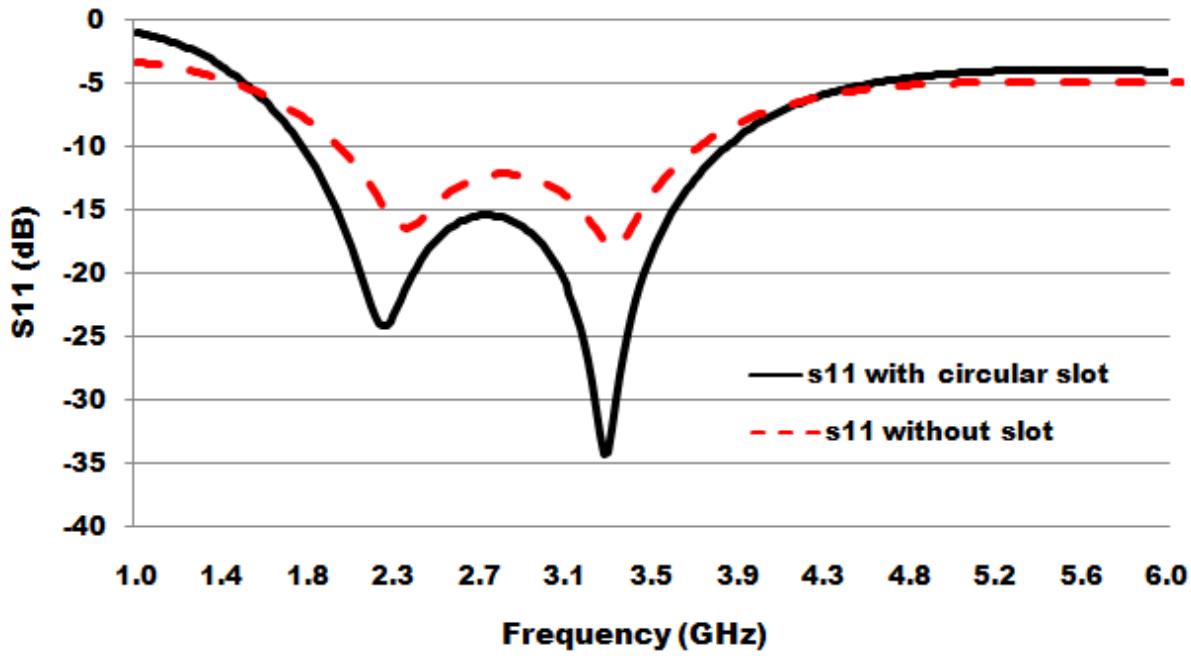

Fig 5.2. Reflection coefficient of the star antenna with and without central circular slot.

It is seen clearly from the comparison that the star antenna with the central circular slot has better matching throughout the -10dB bandwidth when compared to the antenna without the central circular slot. The actual -10dB bandwidth itself however changes very little and there is no major shift in frequency. Therefore the antenna has been matched more efficiently to the 50 ohm source without disturbing the bandwidth.

The main reason behind this enhanced matching is probably due to the fact that the variation of the field distributions along the central circular slot is such that the antenna presents an equivalent impedance which is much closer to 50 ohms and hence the antenna matches more efficiently to the source with very little input power being reflected back.

5.2.2 Parameter sweep for various ground plane dimensions

From the previous section it was noticed that the central circular slot gives rise to enhanced matching. Now, the ground plane dimensions are varied to see which set gives the best antenna parameters.

Initially, keeping the height of the ground structure fixed, the length of the ground plane is varied and a parametric sweep is run to find out the most optimum length of the ground plane (which is considered as 'l'). The various s11 values obtained from the study are presented in the following figure.

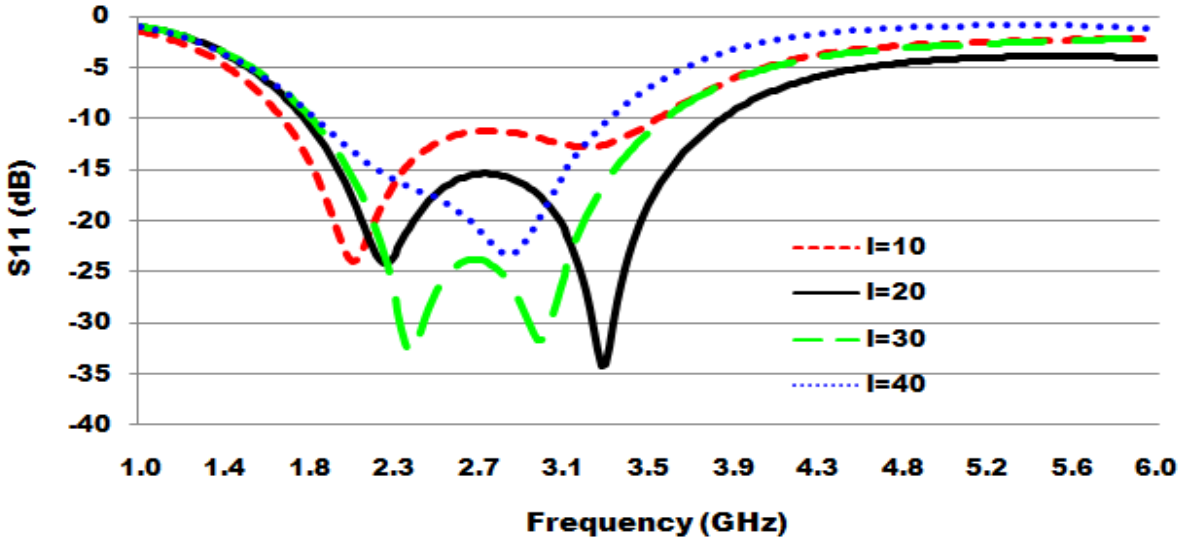

Fig 5.3 S11 vs. freq for four different ground structure lengths.

Clearly it can be seen from the previous figure that the optimum length of the ground plane is indeed the one which has been chosen initially, i.e. l=20mm. This length provides the widest bandwidth among all the four ground plane lengths. Moreover, it also provides good matching throughout the bandwidth from around 1.8 GHz to 4 GHz.

The height of the ground plane is varied similarly and it is found that the height chosen (5 mm) is the height required for good matching, wide bandwidth as well as a return loss curve which covers both the 2.45 GHz and 3.5 GHz which are respectively the WLAN and WiMAX communication channels.

5.3 SIMULATED AND MEASURED S11 OF THE ANTENNA

The analyzed frequency range of the structure is set from 1 GHz to 6 GHz. The s11 graph is shown in Fig. 5.4. VNA model E5071B (300 kHz-8.5GHz) from Agilent Technologies was used to measure s11.

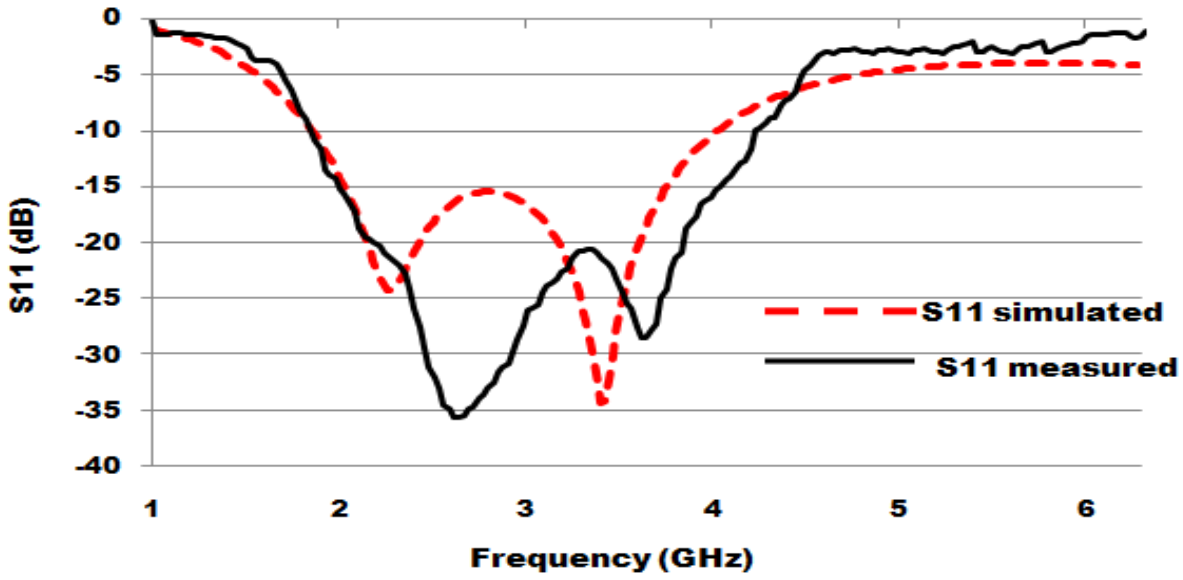

Fig 5.4. Simulated and measured s11 parameters of the designed and fabricated antennas respectively.

There is good agreement between simulated and measured results. The 10 dB bandwidth is measured from 1.8 GHz to 4.2 GHz (2.4 GHz bandwidth) resulting in a percentage bandwidth of 80%. There is also good matching

throughout the 2.4 GHz bandwidth and thus the antenna can cover both the 2.45GHz WLAN band (IEEE 802.11b/g/n) as well as the 3.5 GHz WiMAX band (IEEE 802.16d).

5.4 SIMULATED SURFACE CURRENT DISTRIBUTIONS

The simulated surface current distributions help in identifying the parts of the antenna responsible for radiation for a given frequency. The surface current distributions are shown in the following figures.

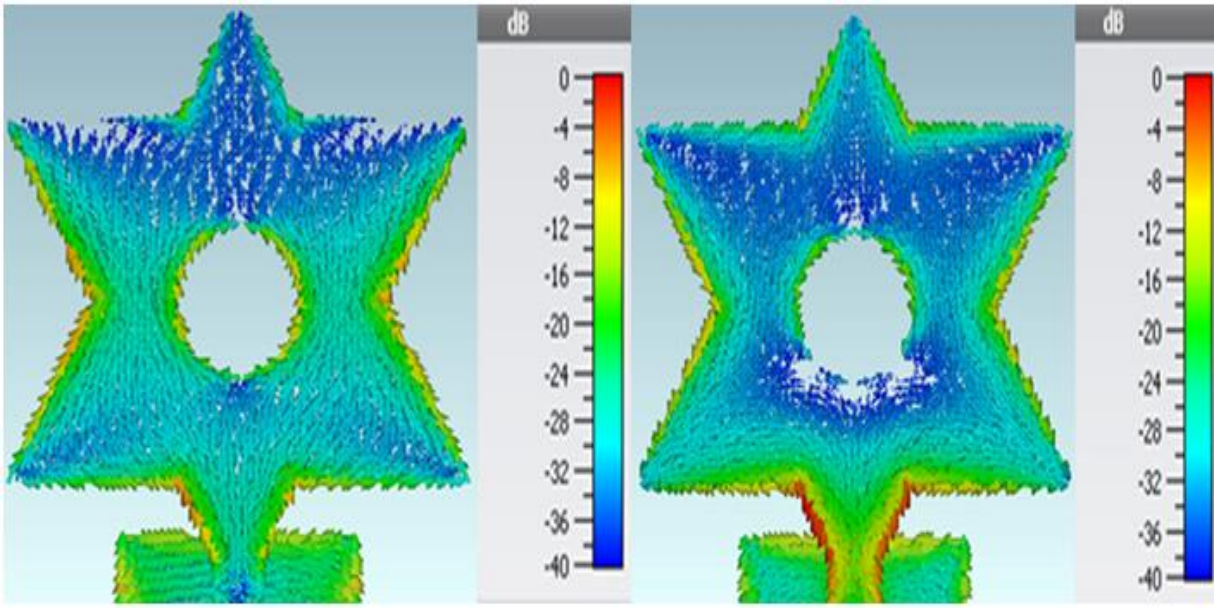

(a) (b)

Fig 5.5. Simulated surface current distributions at (a) 2.45 GHz and (b) 3.5 GHz.

It can be observed that the surface current distributions are similar in both cases. Therefore it can be concluded that the radiation patterns in these frequencies will also be more or less similar.

It will be seen in the next section that this indeed will be the case when the far field radiation patterns are presented.

5.5 SIMULATED AND MEASURED FAR FIELD RADIATION PATTERNS

The far field plots at 2.45 GHz and 3.5 GHz are shown in Fig. 5.6. Transmitter antenna used was 800MHz-18GHz Double Ridged Broadband Horn Antenna (Model HA-08M18G-NF).

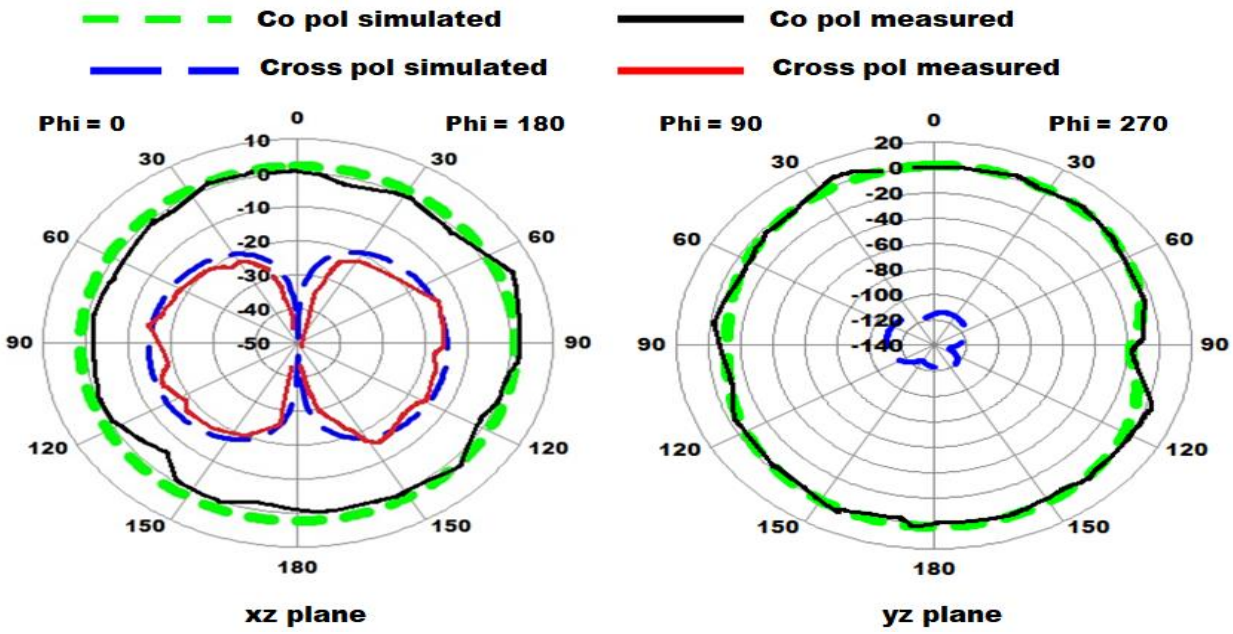

(a)

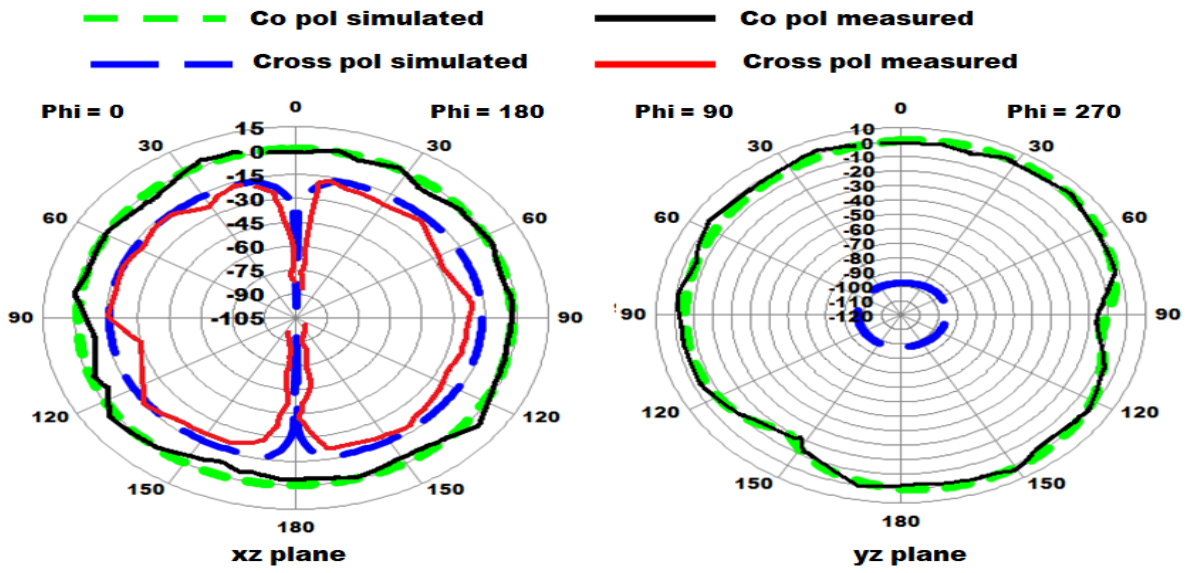

(b)

Fig 5.6 Simulated and measured farfield radiation patterns at (a) 2.45 GHz and (b) 3.5 GHz.

It is observed that in both 2.45 GHz and 3.5 GHz, the antenna shows omnidirectional patterns with low cross polarization levels. The maximum cross polarization levels for 2.45 GHz and 3.5 GHz were found to be -17dBi and -15 dBi in the xz plane respectively. The cross polarization levels in the yz plane for both frequencies were so low (as seen from simulated plots) that they could not be measured due to the lack of such high sensitivity instruments.

The antenna radiation patterns are very similar to that of a dipole antenna with omnidirectional radiation patterns.

5.6 Gain and Efficiency vs. Frequency

The simulated gain and efficiency against frequency graph is shown in Fig. 5.7.

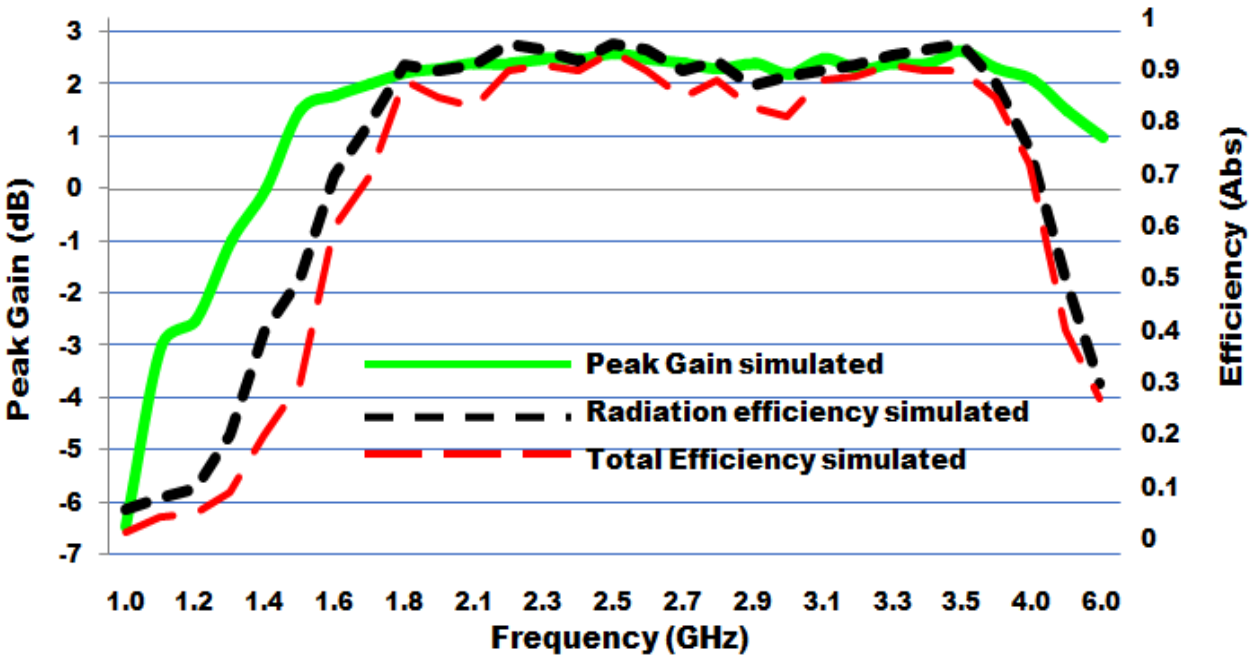

Fig 5.7. Peak gain and efficiency vs. frequency.

The simulated efficiencies at the frequencies of interest are high. The antenna can therefore act as efficient radiators in the frequency regions chosen. The measured peak gain at 2.45 GHz and 3.5 GHz were found to be 2.3 dBi and 2.5 dBi respectively.

5.7 CONCLUSION

A planar wideband star shaped patch antenna is presented with small size, good efficiency, linear polarization and omnidirectional patterns at 2.45 GHz (IEEE 802.11b/g/n, WLAN) and 3.5 GHz (IEEE 802.16d, WiMAX) which are standard IEEE communication channels. The antenna is also small in size, easy and cheap to fabricate and very simple in nature.

REFERENCES

[1] B. H. Ahmad, H. Nornikman," Dual band printed folded dipole antenna for wireless communication at 2.4 GHz and 3.5 GHz applications," 2015 Asia-Pacific Microwave Conference (APMC), 2015, Vol.3, pp.1-3.

[2] I-Fong Chen, Chia-Mei Peng," Printed broadband monopole antenna for WLAN/WiMAX Applications," IEEE Antennas and Wireless Propagation Letters, 2009, Vol.8, pp. 472-474.

[3] Linli Jiang ,Chunlan Lu ,Wenquan Cao ,Changsong Wu ,Feng Yuan, "A dual-band and dual polarized antenna with two nested triangular rings," 2017 Sixth Asia-Pacific Conference on Antennas and Propagation (APCAP), 2017, pp. 1-3.

[4] Daniel Valderas, Juan Ignacio Sancho, David Puente, Cong Ling, Xiaodong Chen, *ULTRAWIDEBAND ANTENNAS: Design and Applications*,2011, Imperial College Press, pp. 157-165, ISBN-13 978-1-84816-491-8 ,10 1-84816-491-2.

CHAPTER - VI

CHARACTERISTIC MODE ANALYSIS OF A FEW SYMMETRIC ENGLISH ALPHABET SHAPED ANTENNAS

6.1 INTRODUCTION

The Characteristic Mode Theory was first derived by R. J. Garbacz in 1968 [1]. It was later modified by Garbacz and Turpin [2]. Harrington and Mautz [3], [4] derived a different method of obtaining the Characteristic Modes which proved to be much simpler and more efficient to perform considering the types of problems at hand.

The Characteristic Mode Theory is a great tool for analyzing and designing PEC bodies, N-port networks, antennas, antennas in multilayered medium, dielectric resonators as well as various antenna systems. The most advantageous part of the Characteristic Mode Analysis (CMA) is that it can predict the various modal characteristics of a designed structure without actually modeling any sources. Therefore, the resulting modes of the CMA are modes which are inherent to the structure itself, without any external excitation or influence.
Characteristic Modes can be defined as a particular set of surface currents and radiated fields that are the characteristics of the obstacle/ body under consideration [1], [2].

The definitions for the characteristic modes show that they constitute a very special orthogonal set in the expansion of any possible induced currents on the surface of the obstacle [4], [5].

Some symmetric English alphabet shaped antennas have been modeled and analyzed using characteristic mode analysis. It has been found by observing the modal significance and far-fields that the significant characteristic modes of each alphabet structure are capable of carrying out communication at their respective resonant frequencies. The English alphabets used in this thesis are: - A, H (or flipped I), M (or inverted W) and N (or flipped Z). Each of these structures can be used as a radiating antenna by providing proper feed at the desired frequency. The alphabet shapes have been found to be efficient radiators at some of the standard IEEE wireless communication standards like the WLAN and/or the WiMAX frequency regions. The antennas have only been studied based on simulation and no fabricated structures have been presented. Therefore this chapter simply deals with the characteristic mode analysis of English alphabet shaped antennas.

The location and choice of feed can be decided by observing the simulated electric field distributions of the radiating modes obtained from the CMA of the structures.

6.2 THEORY OF CHARACTERISTIC MODES FOR PERFECT ELECTRIC CONDUCTING BODIES

The CM analysis gives useful information like (1) resonant frequencies of the inherent modes, (2) modal currents on the surface of the analyzed structure (3) far field modal radiation patterns, and (4) significance of each mode at given frequencies.

The CMA involves solving eigenvalue problem in general. CM can be formulated based on EFIE, MFIE or CFIE. In all the cases, it reduces to solving the generalized eigenvalue equation of the form:-

$$\mathbf{XJ_n} = \lambda_n \mathbf{RJ_n} \qquad (1).$$

With $$\mathbf{X} = \frac{\mathbf{Z} - \mathbf{Z^*}}{2j} \qquad (2),$$

$$\mathbf{R} = \frac{\mathbf{Z} + \mathbf{Z^*}}{2} \qquad (3),$$

$$\mathbf{Z} = \mathbf{R} + j\mathbf{X} \qquad (4).$$

Z is the Method of Moments (MoM) impedance matrix

It can be represented by its Hermitian parts (R) and (X). J_n and λ_n are the real eigenvectors and eigenvalues while n represents the n^{th} order mode.

* represents complex conjugate.

EFIE based CMA can be applied to both open and closed objects. MFIE based CMA is applicable only for closed objects. Most antennas being open structures, EFIE based CMA are used more prevalently.

6.3 IMPORTANT PARAMETERS IN CM ANALYSIS

There are three main parameters to consider during CM analysis:-

- **Eigen values (λ_n)** :-

The total stored field energy within a radiation or scattering problem is proportional to the magnitude of the eigen values.

When $\lambda_n = 0$, the modes are ***externally resonant modes***.

When $\lambda_n > 0$, the stored magnetic field energy dominates, this leads to inductive modes.

When $\lambda_n < 0$, the stored electric field energy dominates, this leads to ***capacitive modes***.

- **Modal significances (M.S)** :-

It is the intrinsic property of each mode. It states the coupling/ interacting capability of each CM with external sources. It measures the contribution of each mode in the total electromagnetic response to a given source. Sometimes it is easier to use the MS other than the eigenvalues to investigate resonance of a structure.

$$MS = \left| \frac{1}{1 + j\lambda_n} \right| \qquad (5).$$

For $\lambda n = 0$, M.S = 1. Modes having M.S > 0.707 are usually efficient radiating modes.

- **Characteristic Angle (α_n)** :-

The CM theory defines a set of real characteristic currents on the surface of a body. Each of these currents radiates a characteristic field in free space. The phase lag between the real currents and the fields gives us the characteristic angles.

$$\alpha_n = 180° - \tan^{-1} \lambda_n \qquad (6)$$

It provides a way to better show the mode behaviour near resonance.

For $\alpha_n = 180^0$, the mode associated will be ***externally resonant***.

For $90^0 < \alpha_n < 180^0$, the mode associated will be ***inductive***.

For $180^0 < \alpha_n < 270^0$, the mode associated will be ***capacitive***.

The 3dB bandwidth of the modes can be considered from 135^0 to 225^0.

The advantages of carrying out Characteristic Mode Analysis of PEC bodies includes (but is not limited to) the following:-

- A physical understanding of the various inherent modes of the structure is available along with the current distributions near those modes and far fields produced.
- Locations of feed can be identified at places having maximum current densities.
- The behaviour of the modes with frequency can be studied and the structure under consideration can be used accordingly.
- Circular polarization can be achieved by exciting two modes having same modal significance and characteristic angles difference of 90° at the frequency of interest.

6.4 DESIGNED ANTENNA STRUCTURES

The following antenna structures were designed using CST STUDIO SUITE®.

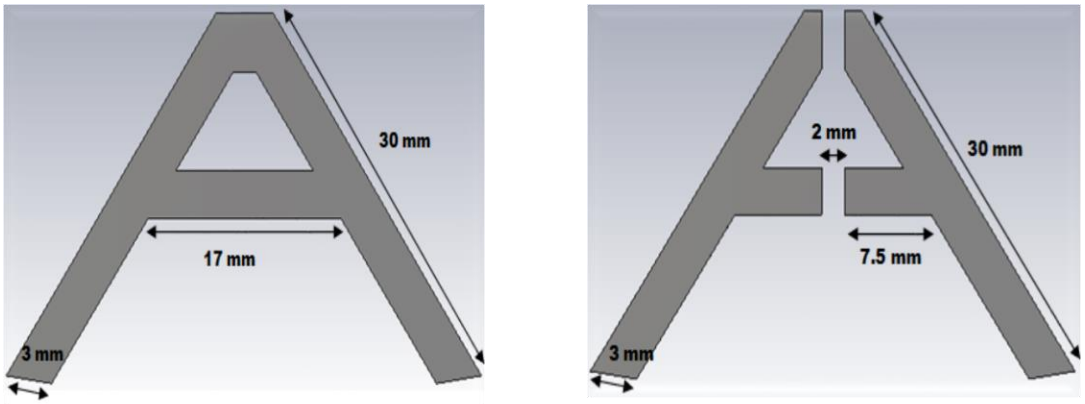

(a)

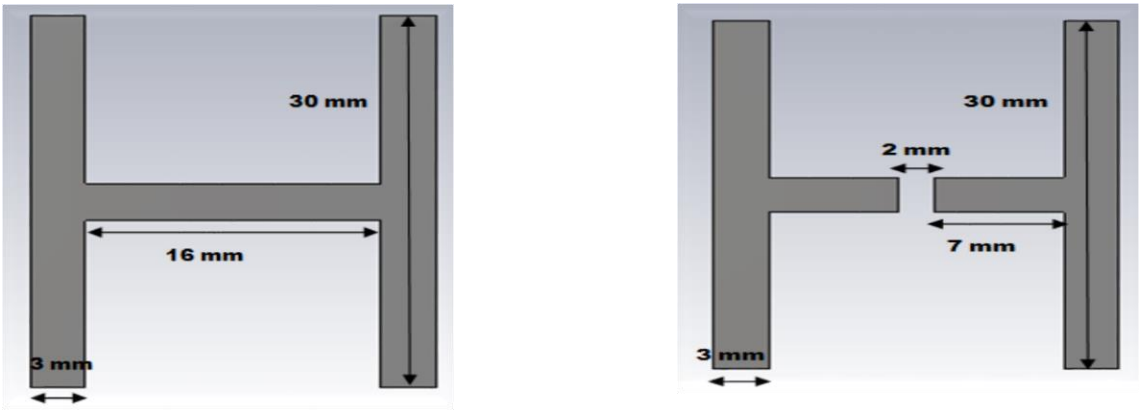

(b)

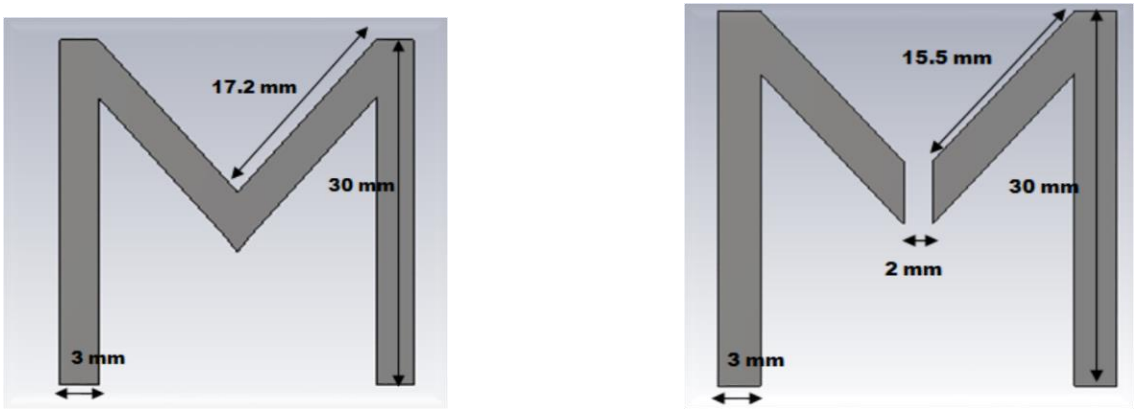

(c)

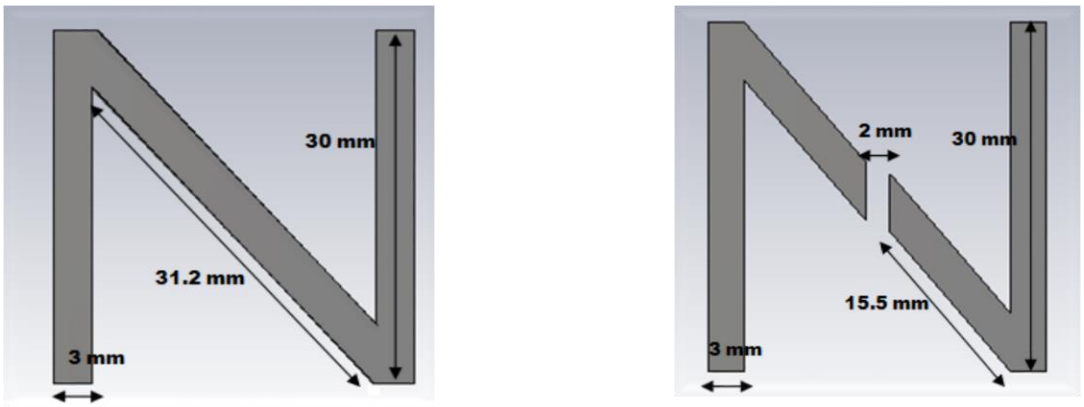

(d)

Fig 6.1 The designed alphabet antennas. (a) Full and Separated A, (b) Full and separated H, (c) Full and Separated M and (d) Full and Separated N.

6.5 CHARACTERISTIC MODE ANALYSIS

The CMA of the designed antennas has been performed using CST Studio Suite® with the thickness of PEC bodies chosen as 1 mm. Mode tracking was enabled to identify clearly the modes with varying frequency. The chosen range of analysis was from 1GHz to 10GHz and the first three modes within this range have been studied. Mesh size was chosen as lambda/15 for good accuracy. The antennas are simple PEC sheets of thickness 1mm as stated above.

6.5.1 LETTER A

- **Eigenvalues**

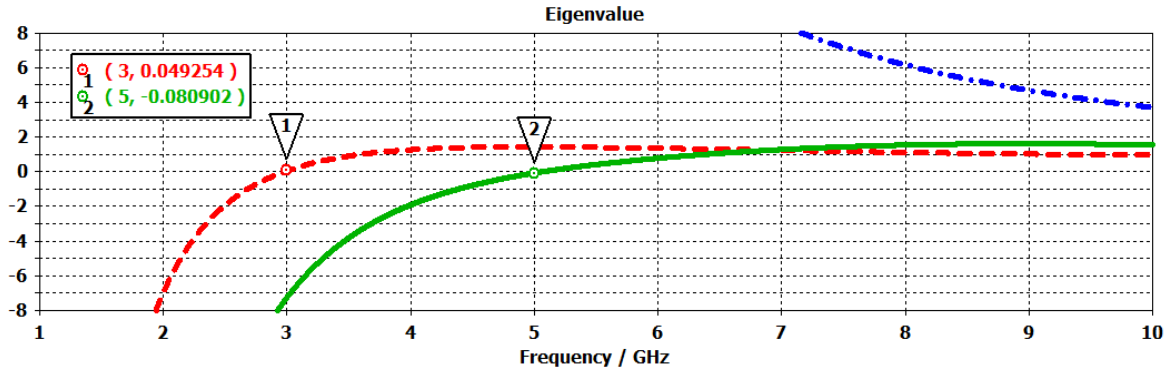

Full A

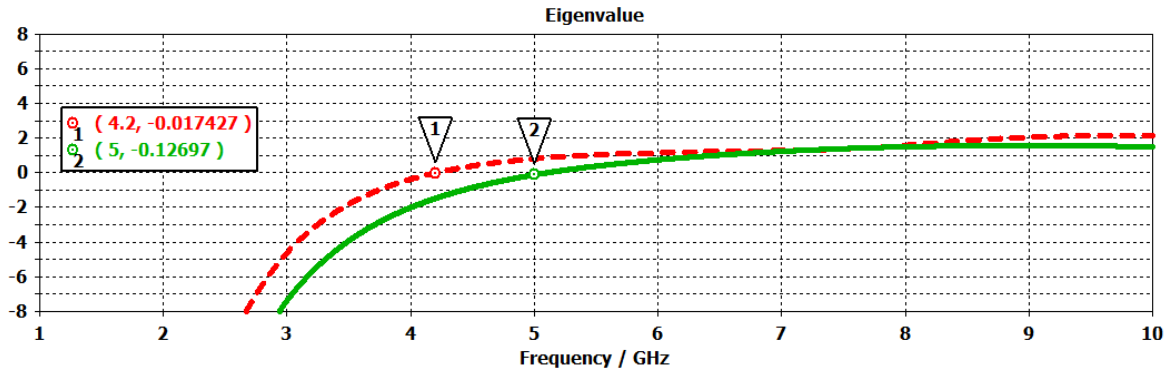

Separated A

Fig 6.2. Letter A Eigenvalue vs. frequency.

It can be seen that for both the structures, only two significant modes are excited within this frequency range.

- **Modal Significance**

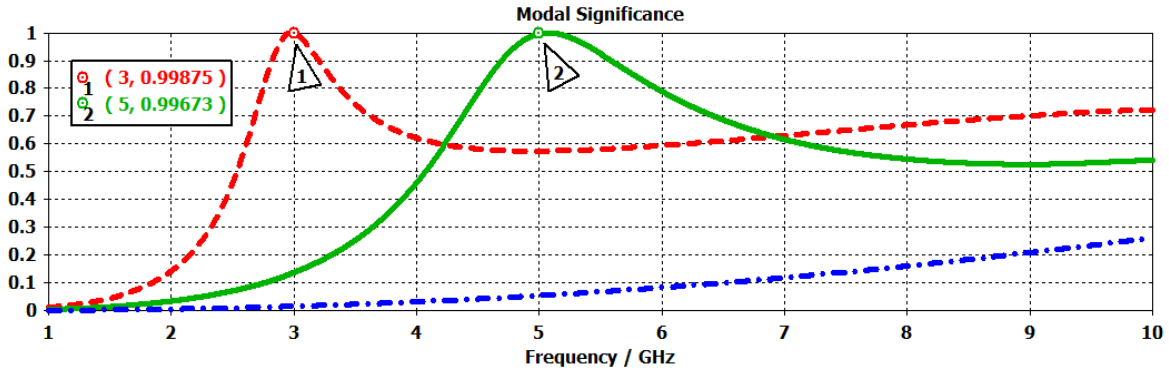

Full A

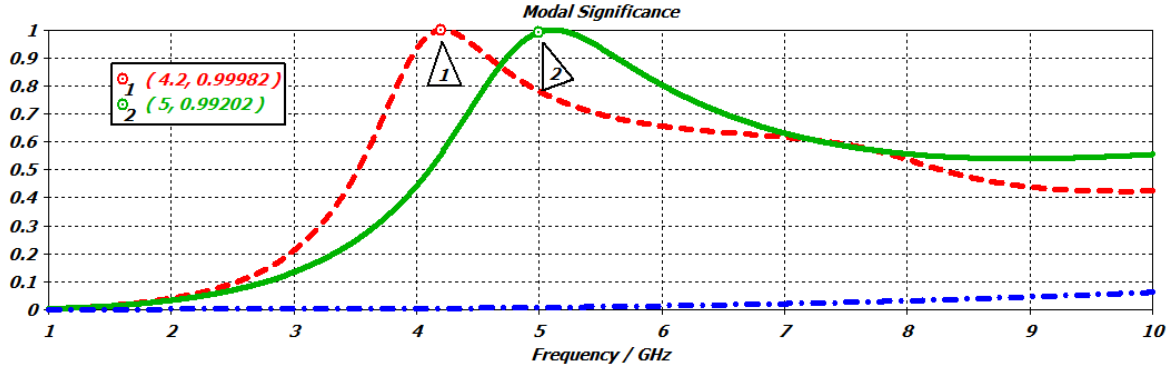

Separated A

Fig 6.3. Letter A Modal significance vs. frequency.

From the figure it can be seen that the corresponding peaks of the two modes from the marked frequencies. It is seen that the Full A covers the 3.5 GHz region and 5.2 GHz regions while the Separated A covers the 5.2 GHz region only.

- **Characteristic Angles**

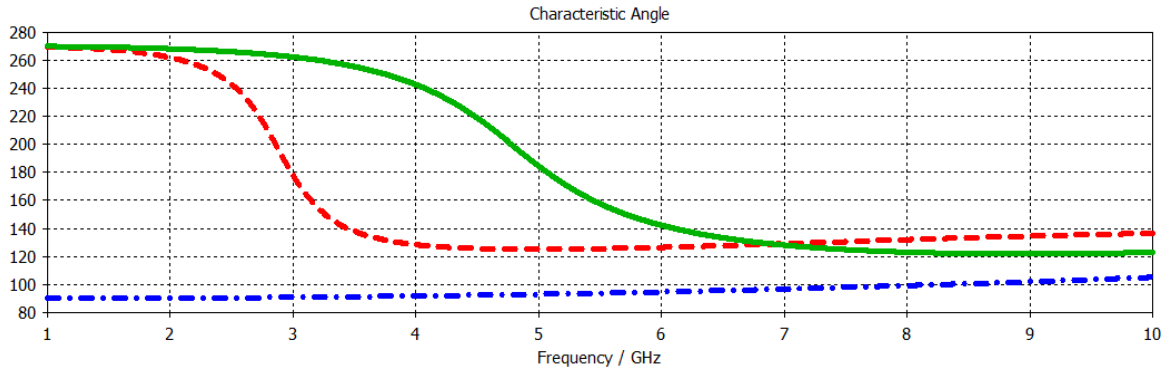

Full A

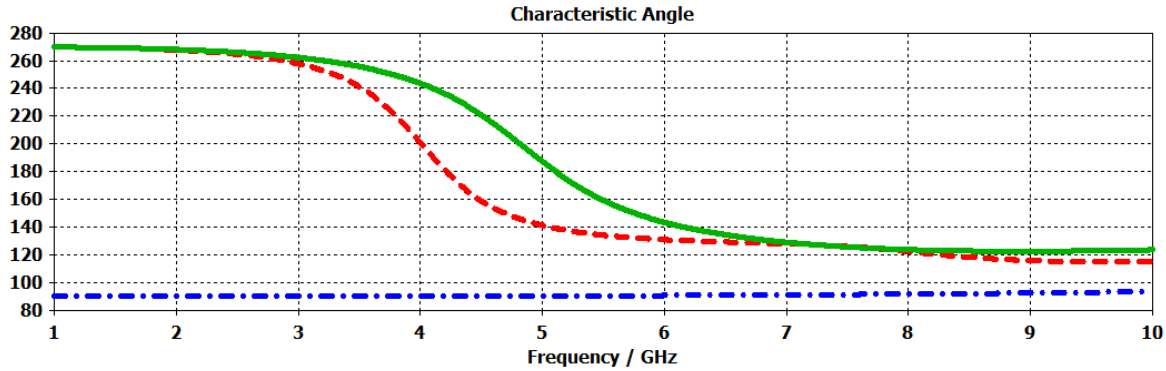

Separated A

Fig 6.4. Letter A Characteristic Angle vs. frequency.

For both the antennas, the two significant modes start off as being capacitive and gradually after resonance become inductive. The third insignificant mode remains inductive throughout and hence there is energy storage for this mode.

- **Modal Current Distributions**

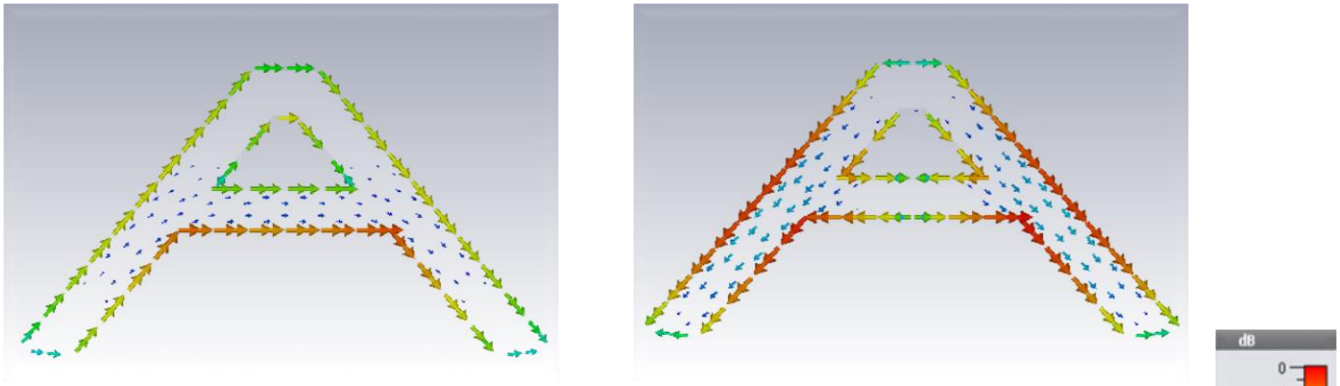

3.5 GHz 5.2 GHz

Full A

4.2 GHz 5.2 GHz

Separated A

Fig 6.5. Modal current distributions of Letter A.

It can be seen that there is a shift in first mode frequency from the full A antenna to the separated A antenna because the path length of the primary mode current has been shortened by the introduction of the separation through the middle. This separation therefore changes the modes where there are current maximas near the middle of the structures which cannot exist once the structure is separated through the middle. The 5.2 GHz mode is same for both the antennas since there is naturally a current minima near the separation axis and hence the separation does not affect the current distributions much. It will be seen that due to unchanged current distribution, the modal far field patterns will be the same for both antennas at 5.2 GHz.

- **Modal Far Field Directivity patterns**

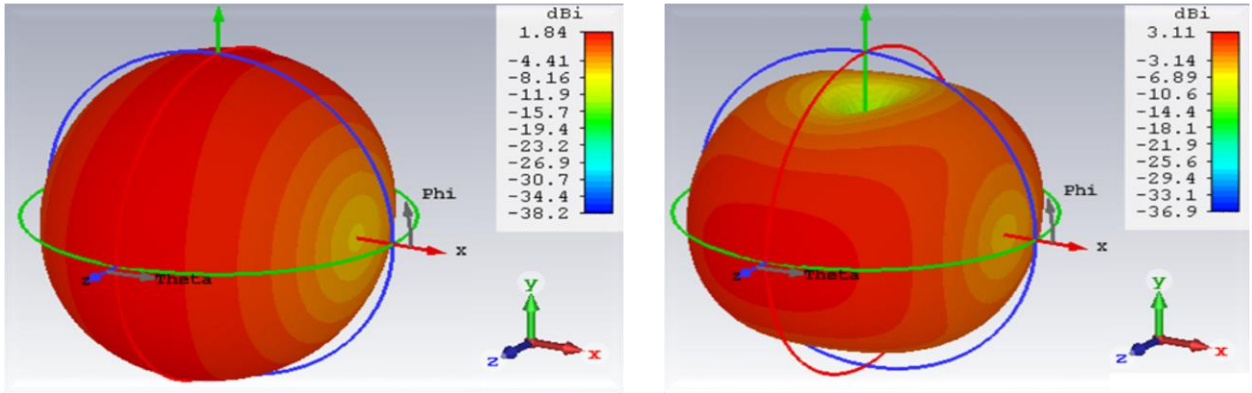

3.5 GHz 5.2 GHz

Full A

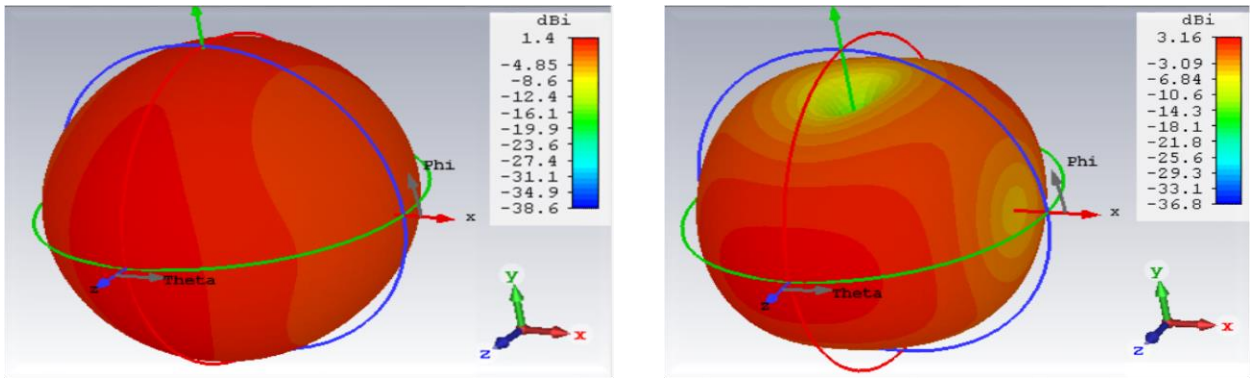

4.2 GHz 5.2 GHz

Separated A

Fig 6.6. Modal far field directivity patterns of Letter A.

As discussed in the previous section, the 1st mode of the two antennas (3.5GHz and 4.2GHz) has different patterns due to different current distributions whereas the 5.2 GHz mode is identical for both the full A and the separated A.

6.5.2 LETTER H

- **Eigenvalues**

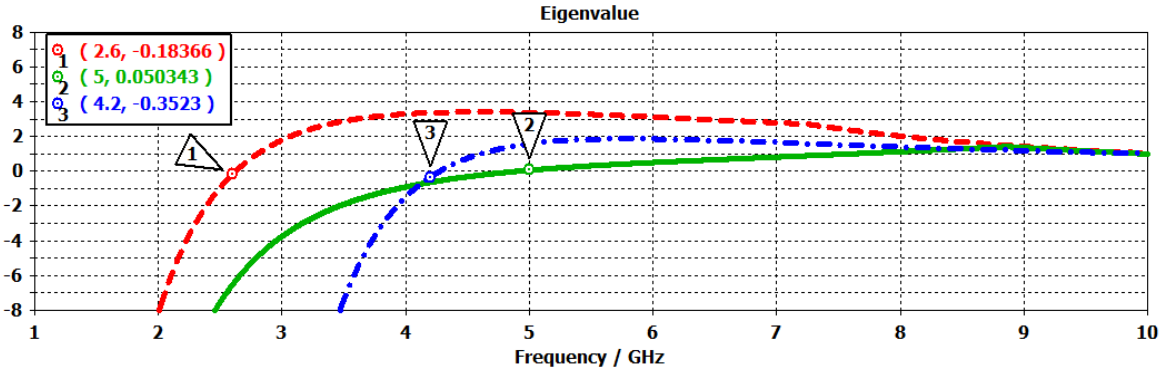

Full H

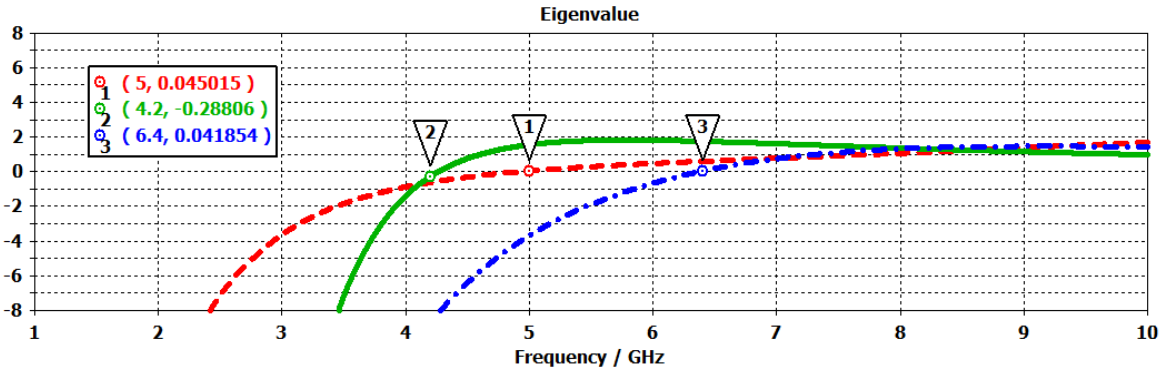

Separated H

Fig 6.7. Letter H Eigenvalue vs. frequency.

It can be seen that all three modes can be excited significantly within the frequency range studied. Full H antenna covers the 2.5 GHz region and 5.2 GHz region whereas the separated H again has a primary mode frequency shift (from 2.6 GHz to 4.2 GHz) and covers the 5.2 GHz frequency region.

- **Modal Significance**

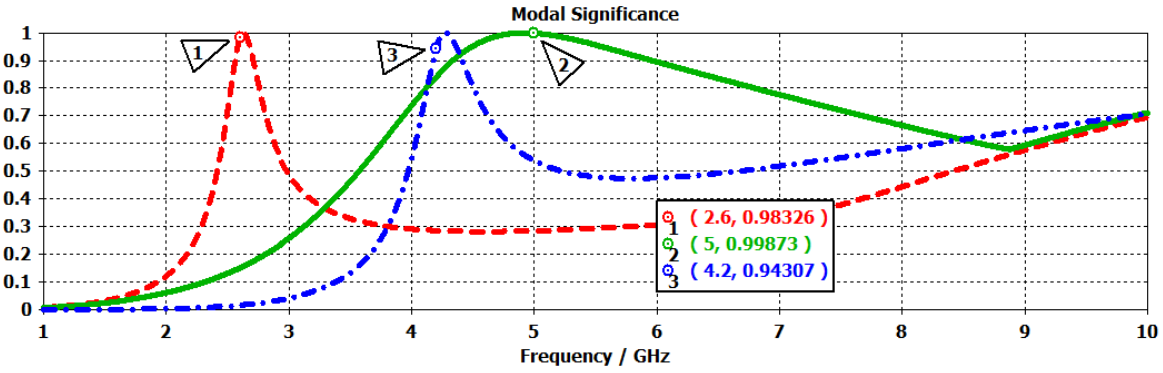

Full H

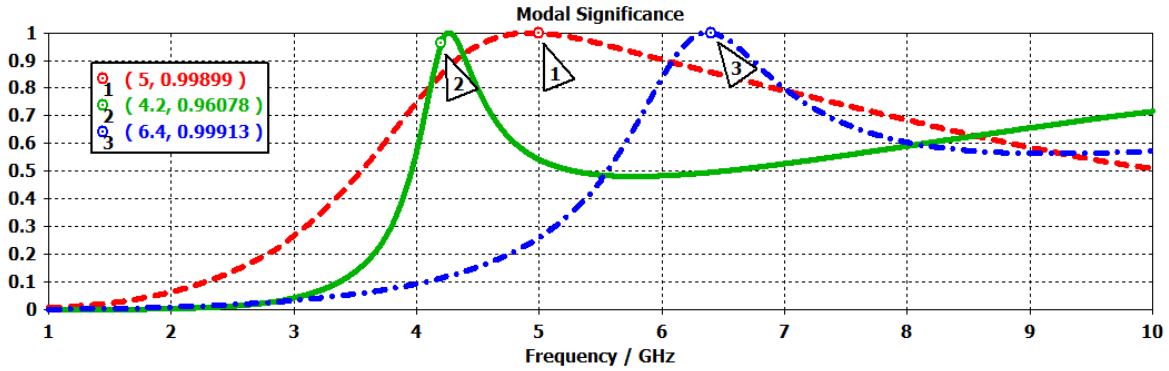

Separated H

Fig 6.8. Letter H Modal Significance vs. frequency.

The information from the modal significance curves confirms the eigenvalue study conclusions with the full antenna covering the 2.5 GHz and 5.2 GHz while the separated antenna covers the 5.2 GHz regions.

- **Characteristic Angle**

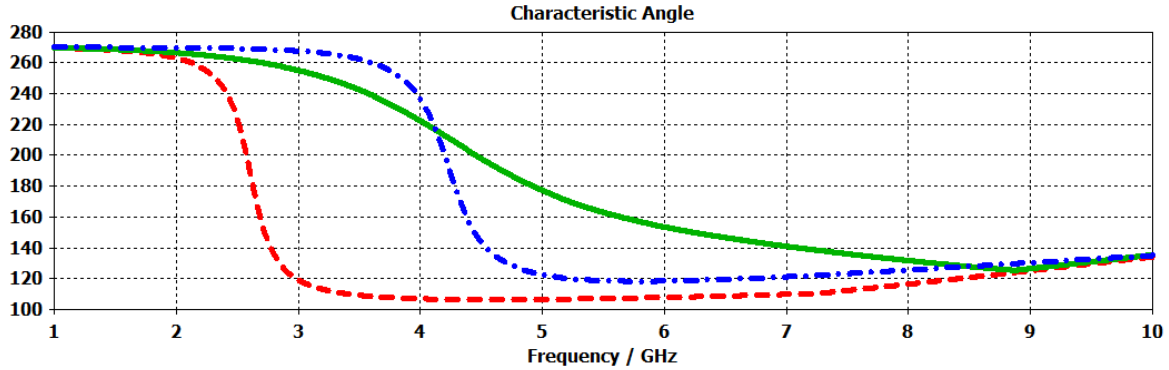

Full H

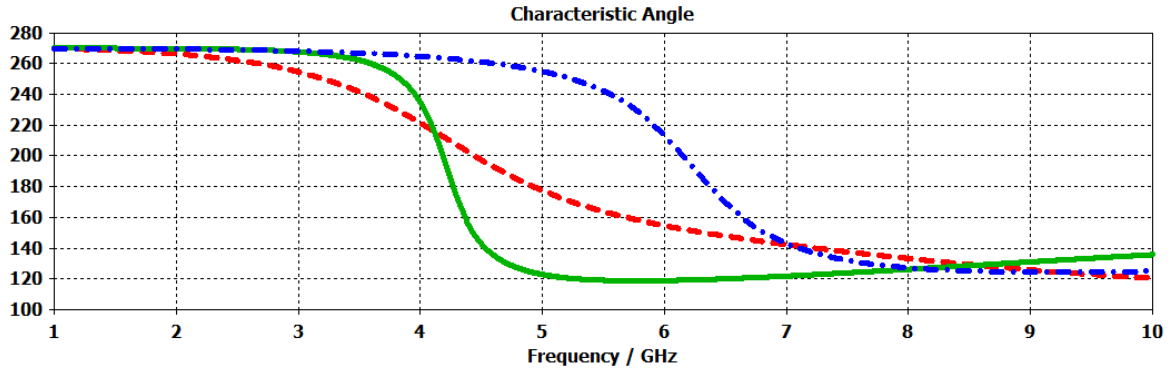

Separated H

Fig 6.9. Letter H Characteristic Angle vs. frequency.

For both the antenna structures, the three modes initially start off as being capacitive, then after resonating they end up being inductive in nature.

- **Modal Current Distributions**

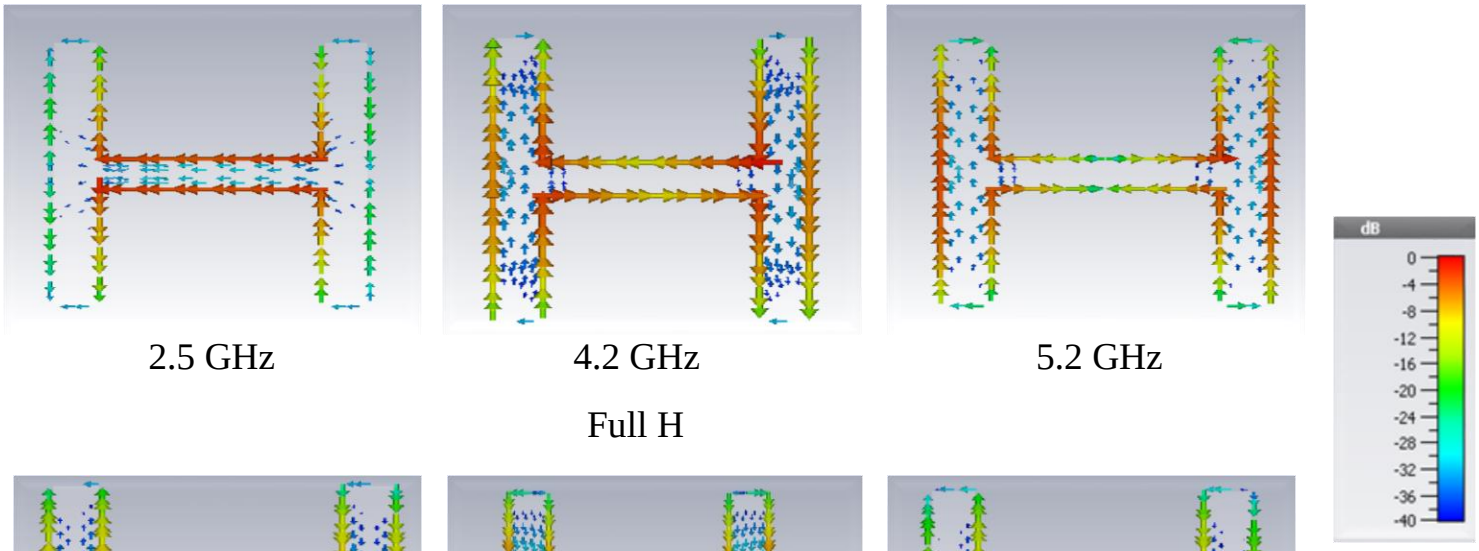

2.5 GHz 4.2 GHz 5.2 GHz

Full H

4.2 GHz 5.2 GHz 6.4 GHz

Separated H

Fig 6.10. Modal current distributions of Letter H.

It can again be seen that modes having current maximas near the separation axis in the full structure cannot exist in the separated structure. Current distributions being moderate and minimum for the 4.2 GHz mode and 5.2 GHz modes, they are present for the separated structure as well. But the 2.5 GHz mode has a current maximum near the centre for the full H, therefore this mode does not exist for the separated H structure and we get a different mode at 6.4 GHz.

- **Modal Far Field Directivity patterns**

The modal far field directivity patterns for the three significant modes of the full H and separated H antennas are presented in the following page. It shall be seen that the 4.2 GHz and 5.2 GHz modes for both the antennas share similar radiation patterns since they possess similar surface current distributions as seen from the previous section. The 2.5 GHz mode is similar to that of a horizontal dipole while the 6.4 GHz mode is a somewhat distorted version of the 2.5 GHz mode.

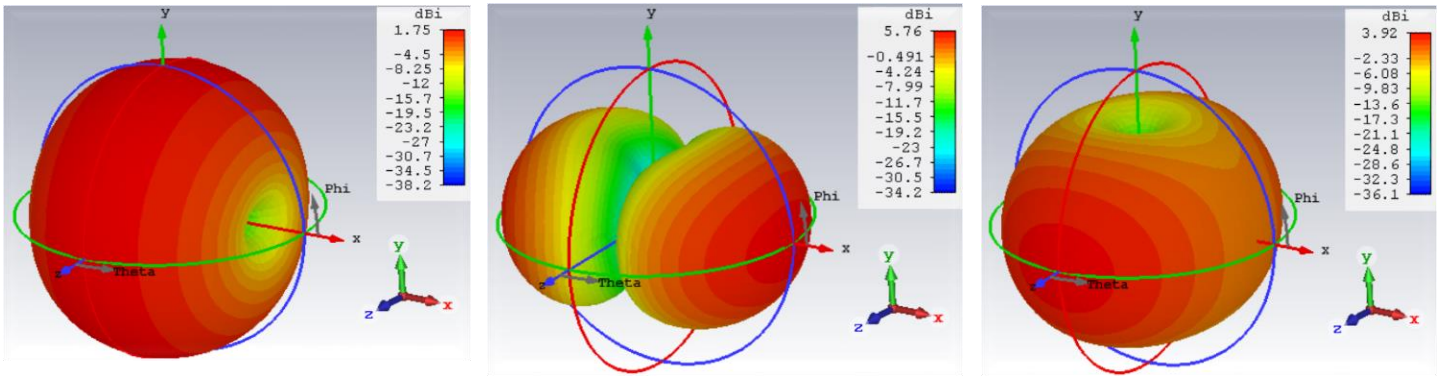

2.5 GHz 4.2 GHz 5.2 GHz

Full H

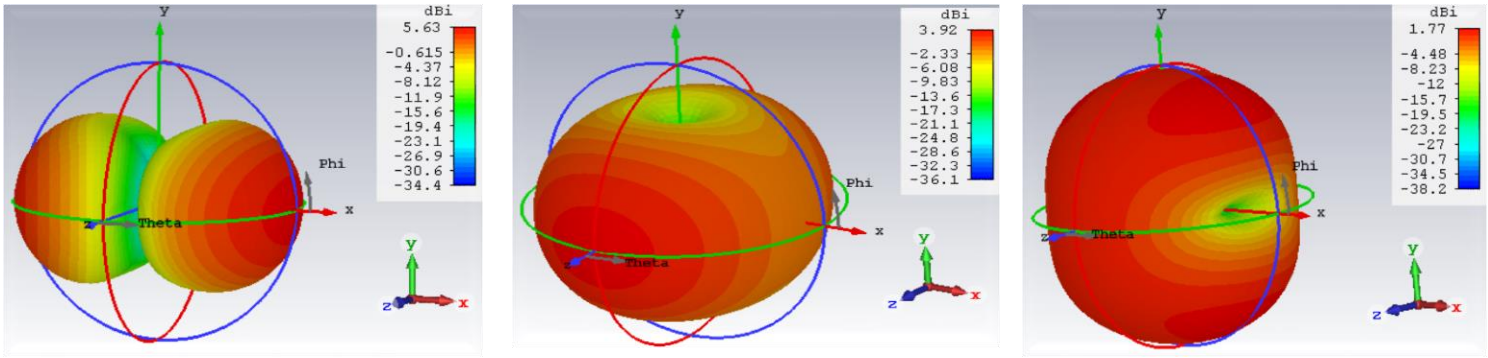

4.2 GHz 5.2 GHz 6.4 GHz

Separated H

Fig 6.11. Modal far field radiation patterns of the Letter H.

6.5.3 LETTER M

- **Eigenvalue**

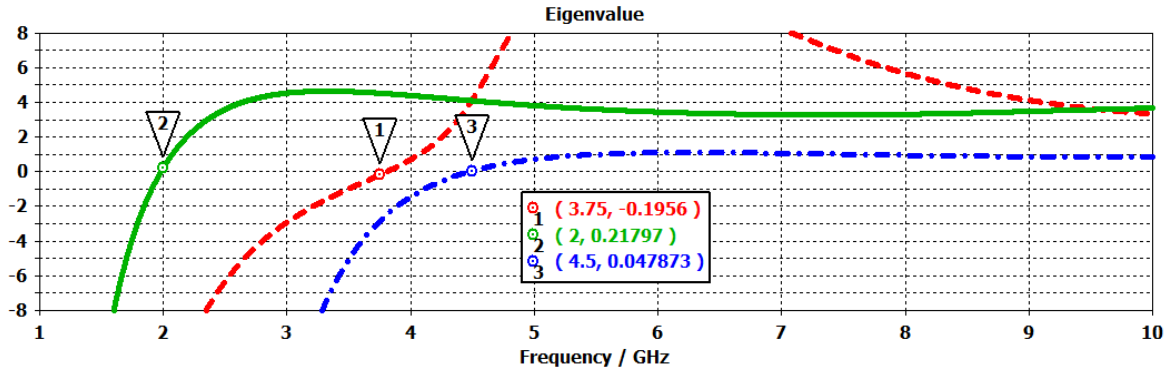

Full M

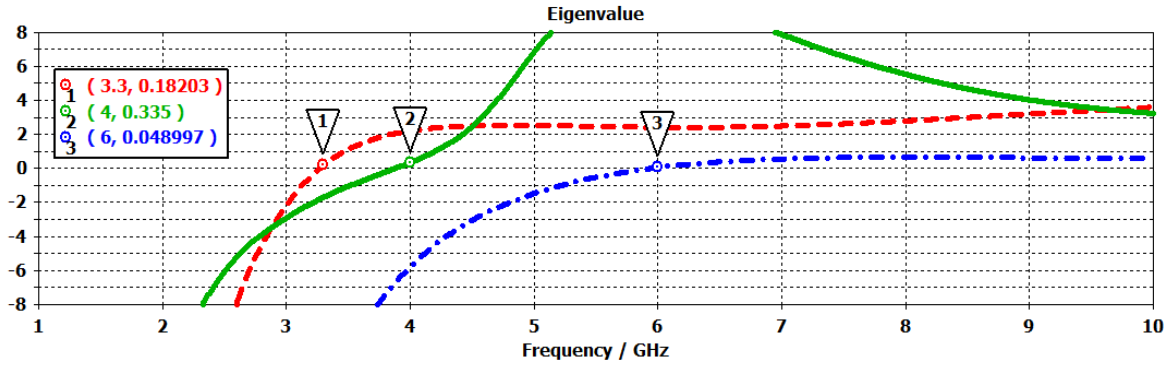

Separated M

Fig 6.12. Letter M Eigenvalues vs. frequency.

All the three modes can be excited for both the structures. Both the structures cover the 3.5 GHz frequency region.

- **Modal Significance**

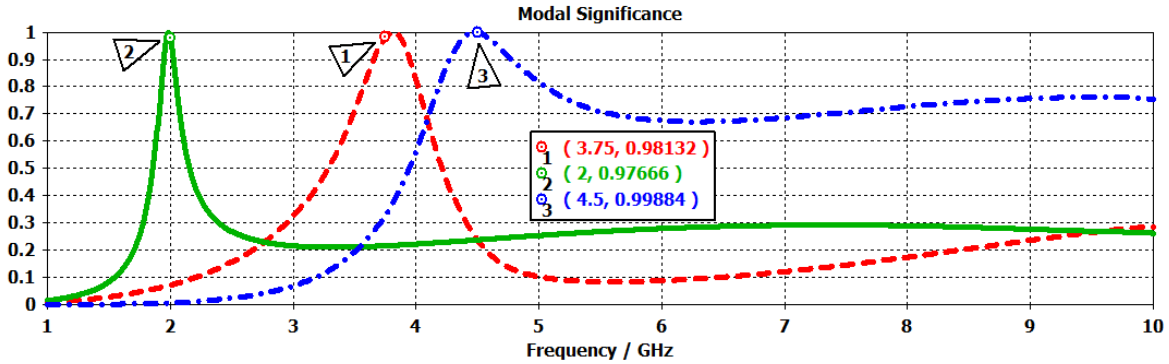

Full M

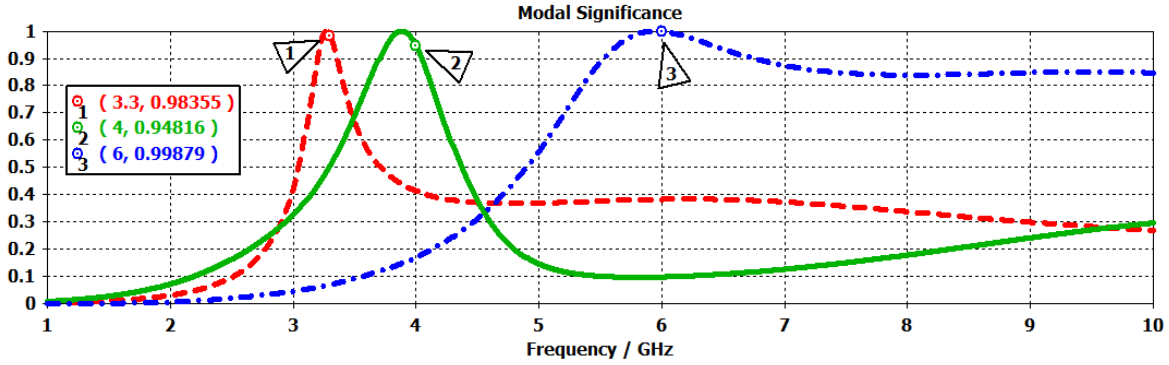

Separated M

Fig 6.13. Letter M Modal Significance vs. frequency.

The peaks of the corresponding modes of both the structures are shown in the figures. It is confirmed that both the antennas can cover the 3.5 GHz frequency region.

- **Characteristic Angle**

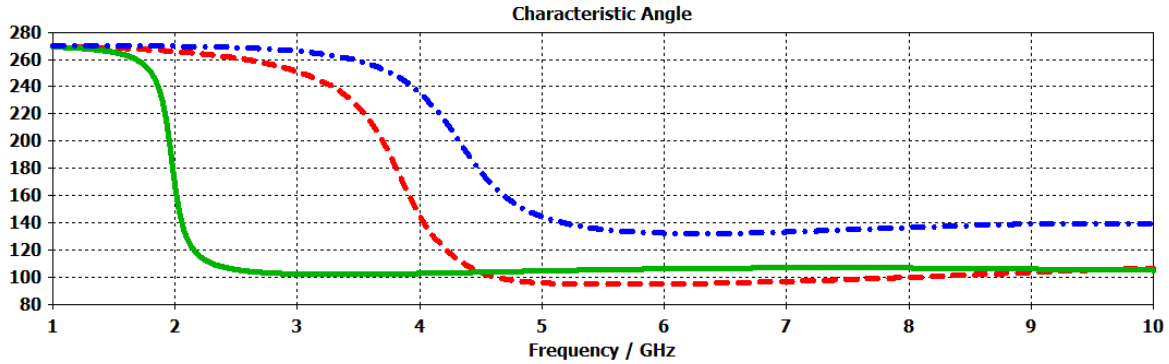

Full M

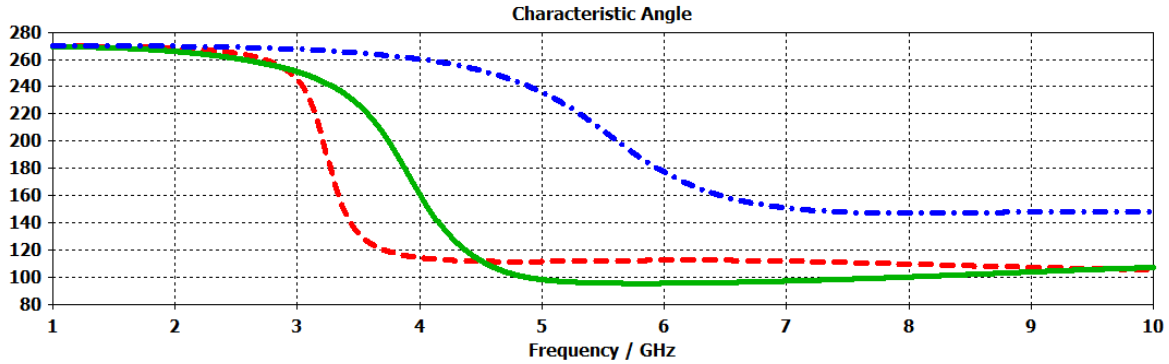

Separated M

Fig 6.14. Letter M Characteristic Angle vs. frequency.

The modes for both the structures start off as being capacitive and after resonance they end up being inductive. This phenomenon is similar to the characteristic angles for the previous cases.

- **Modal Current Distributions**

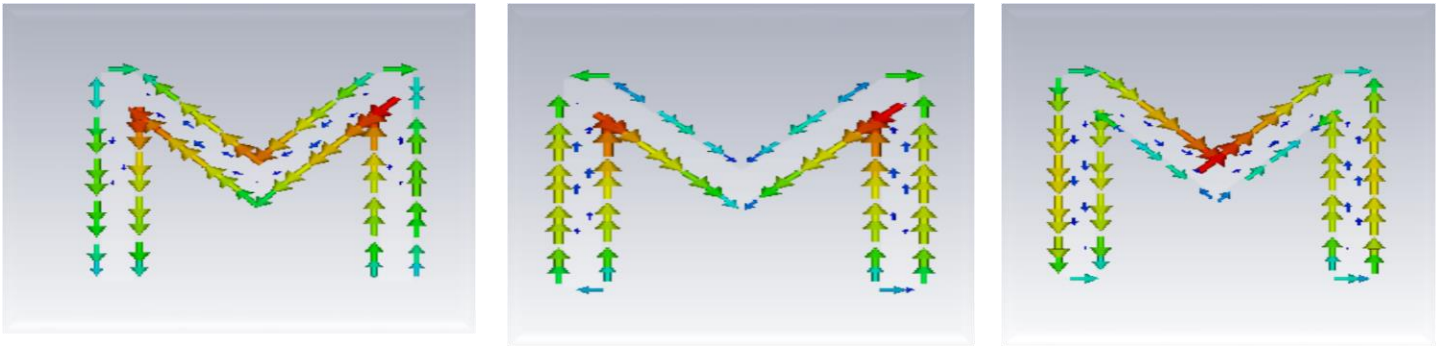

2 GHz 3.5 GHz 4.5 GHz

Full M

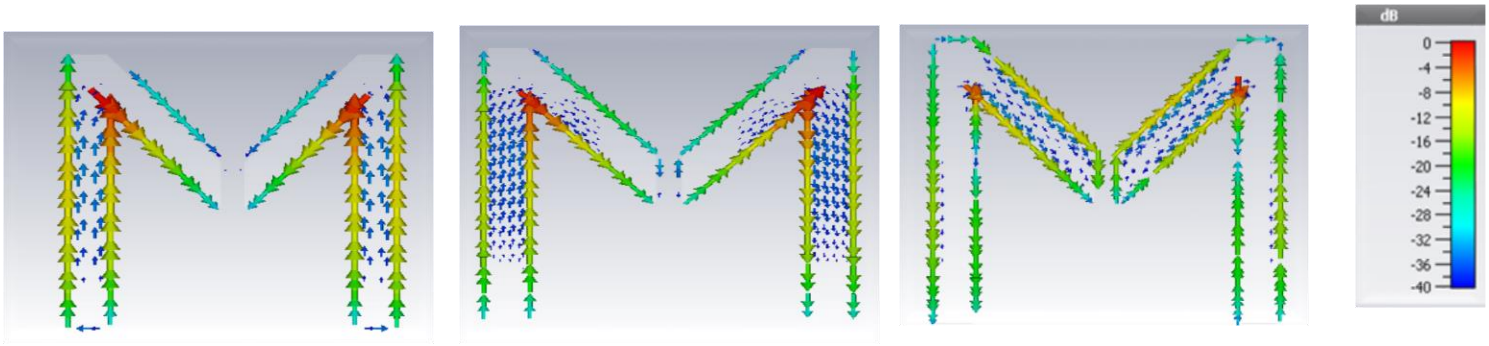

3.5 GHz 4 GHz 6 GHz

Separated M

Fig 6.15. Modal current distributions for Letter M.

It can be seen that except the 3.5 GHz mode where there is a current minima at the centre line, all the other modes are different for both the structures since there are current maximas along the central line for the other two modes of the full M which cannot exist for the separated M.

- **Modal Far Field Directivity pattern**

  The far field radiation patterns of the modes at the selected frequencies are shown. It can be seen that the 3.5 GHz mode is indeed similar for both the full M and separated M structures and has maximum directivity along the positive and negative z axis.

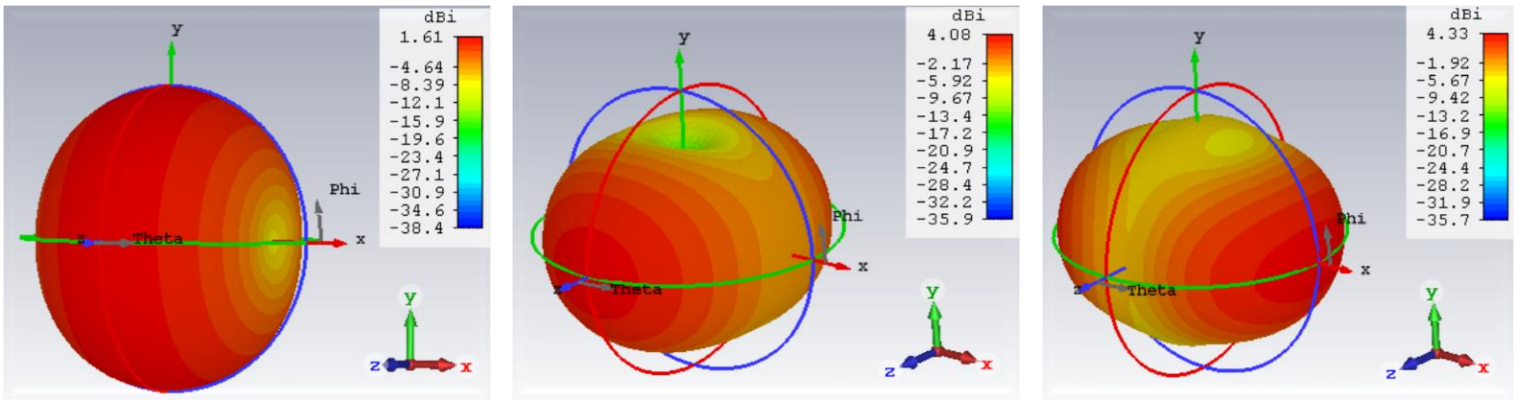

2 GHz 3.5 GHz 4.5 GHz

Full M

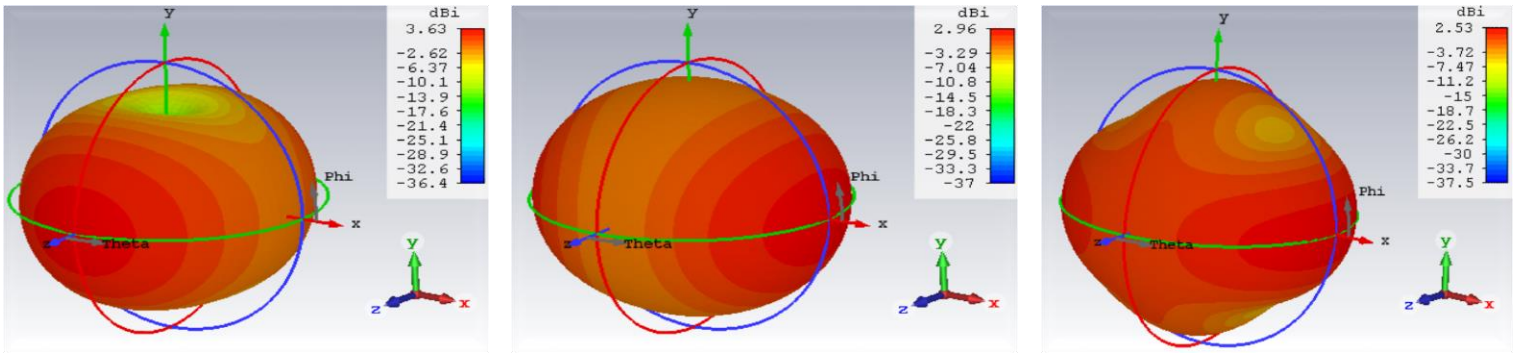

3.5 GHz 4 GHz 6 GHz

Separated M

Fig 6.16. Modal far field radiation patterns for the Letter M.

It is seen that the radiation patterns at the 3.5 GHz regions are same indeed for both the antennas while the others are all dissimilar due to difference in the modal current distributions.

6.5.4 LETTER N

- **Eigenvalues**

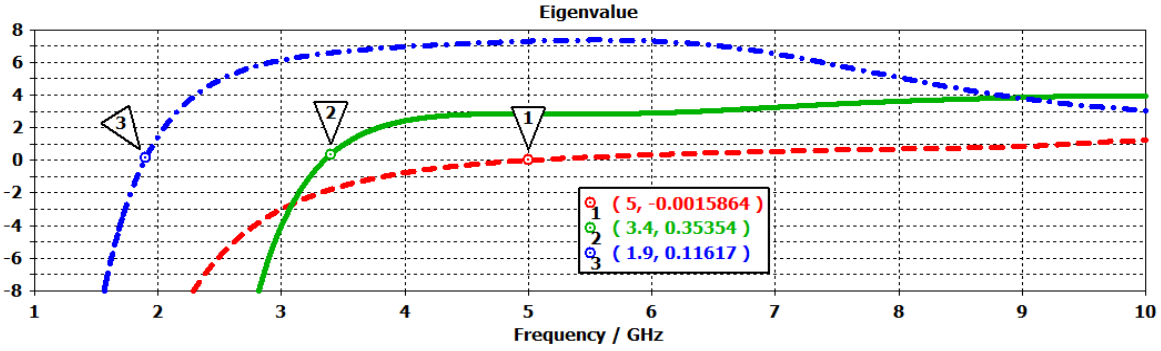

Full N

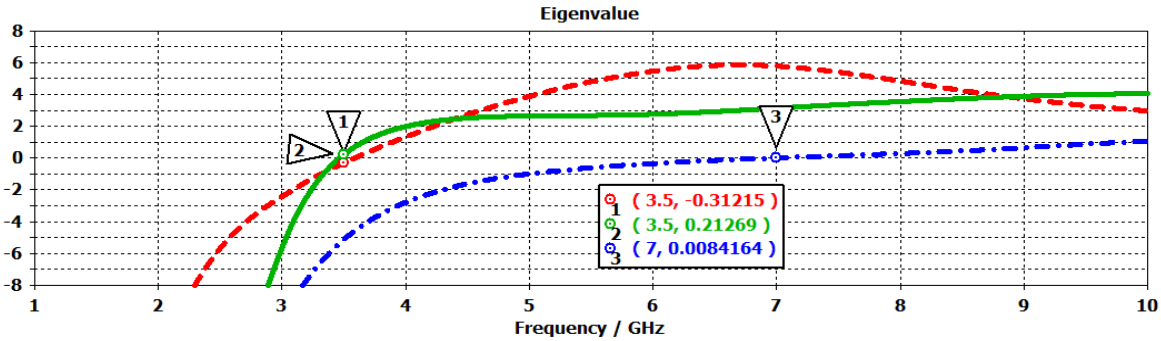

Separated N

Fig 6.17. Letter N Eigenvalues vs. frequency.

It can be seen that the three modes can be excited significantly for both the structures. For the separated N structure, it can further be seen that the first two modes (at 3.5 GHz) are excited at the same frequency.

- **Modal Significance**

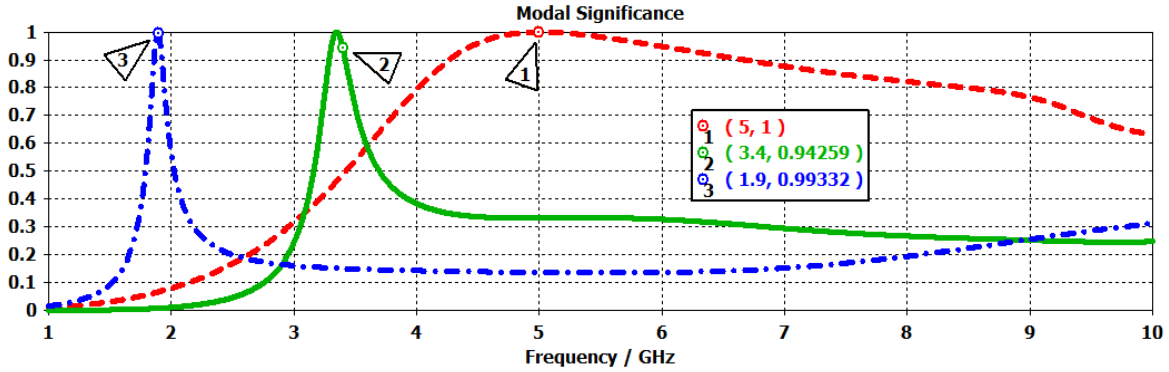

Full N

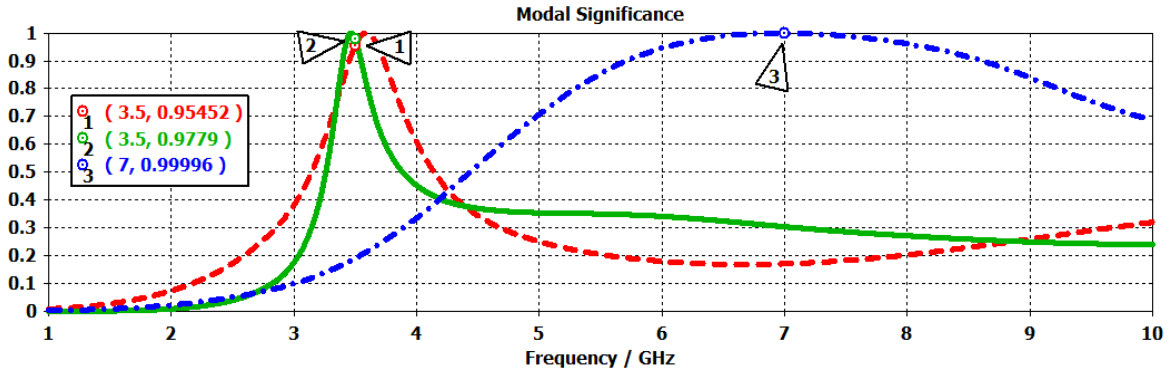

Separated N

Fig 6.18. Letter N Modal significance vs. frequency.

It can be seen from the modal significance curves that for the separated N, the 1st two modes have same magnitude at 3.5 GHz. Hence, if the characteristic angle between these two modes is found to be 90^0, then the modes could be excited simultaneously to attain circular polarization. This issue is addressed in the following section. The full N antenna is seen to cover the 3.5 GHz and 5.2 GHz regions while the separated N covers the 3.5 GHz region and 5.2 GHz region.

- **Characteristic Angle**

From the characteristic angle plots shown in the following page, it is seen that the two modes of the separated N which occur at 3.5 GHz have a characteristic angle difference between them of around 30^0 only. Hence, they cannot be excited simultaneously to get circular polarization. Apart from that, it is found

that in both the structures, the modes start off as being capacitive, then resonate and finally end up being inductive as frequency increases.

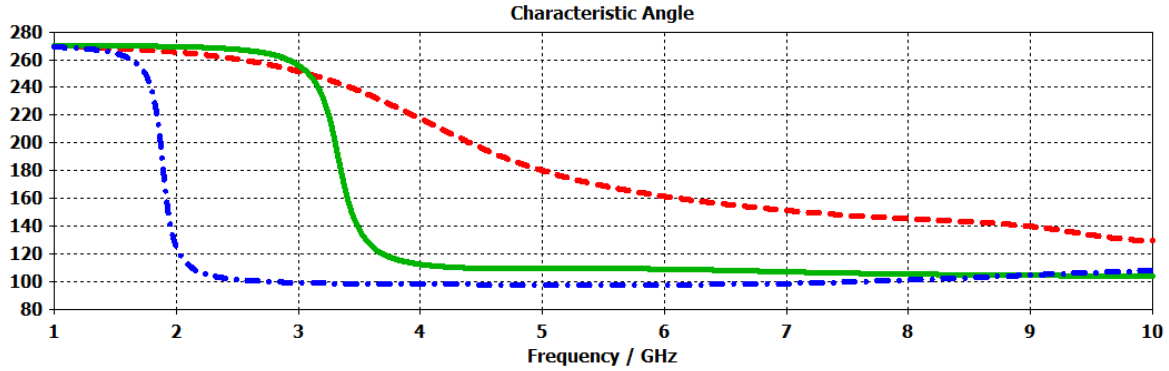

Full N

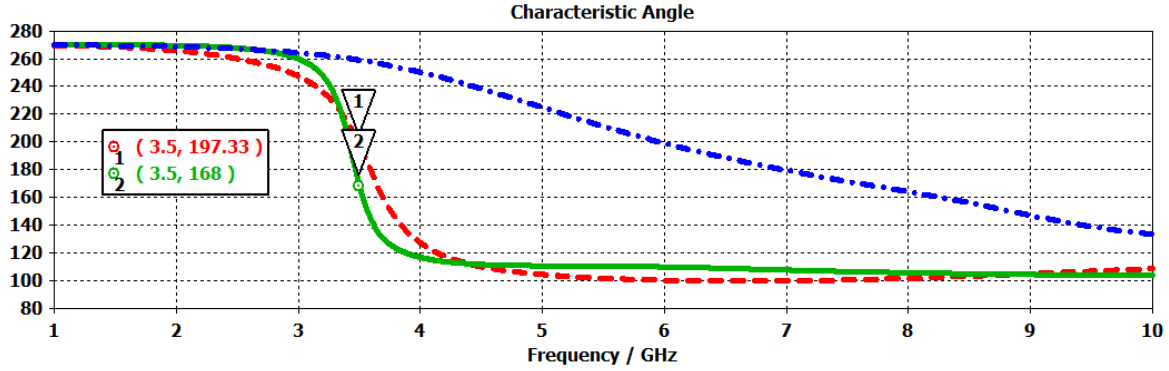

Separated N

Fig 6.19. Letter N Characteristic Angle vs. frequency.

- **Modal Current Distributions**

It can be seen that there are 3.5 GHz modes for both the full N and separated N and the separated N even has two modes both excited at 3.5 GHz. This mode initially has a current minima near the separation axis and hence can exist in the separated N structure along with the initial full N structure.

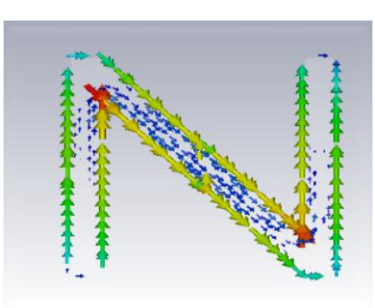

1.9 GHz

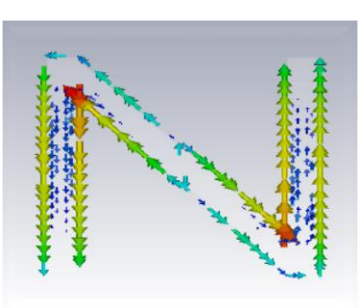

3.5 GHz

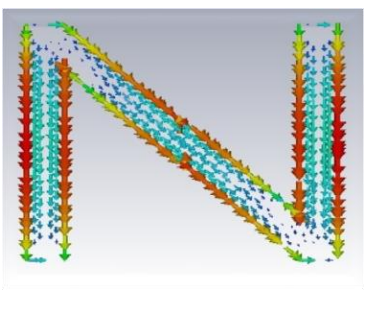

5.2 GHz

Full N

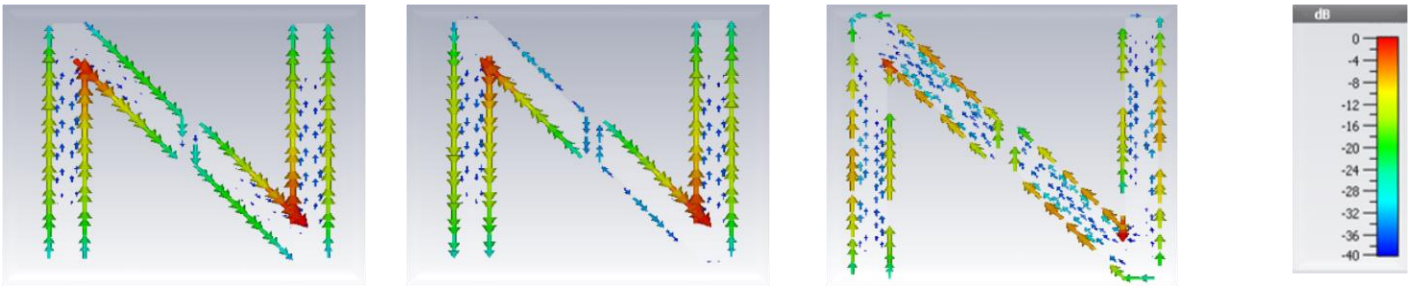

3.5 GHz 3.5 GHz 7 GHz

Separated N

Fig 6.20. Modal Current Distributions for the Letter N.

- **Modal Far Field Directivity patterns**

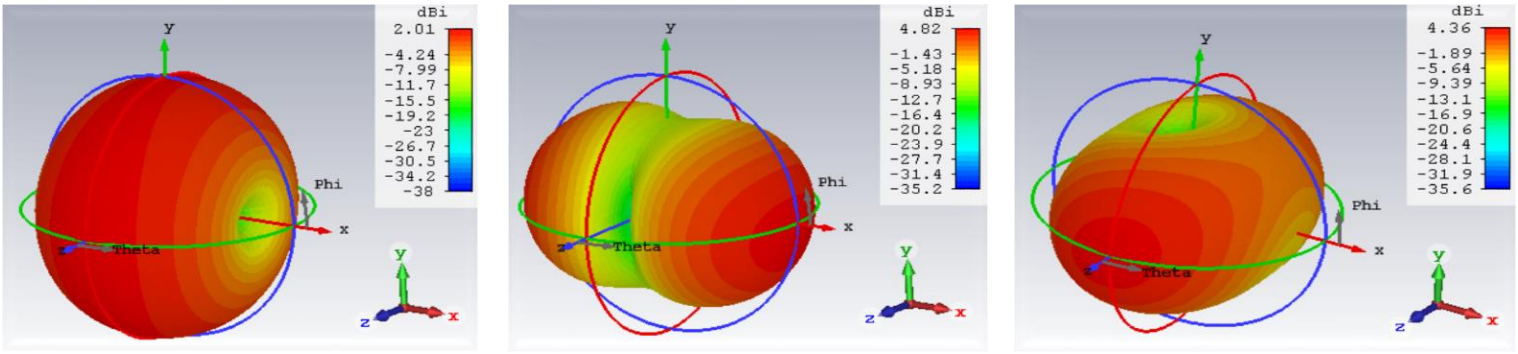

1.9 GHz 3.5 GHz 5.2 GHz

Full N

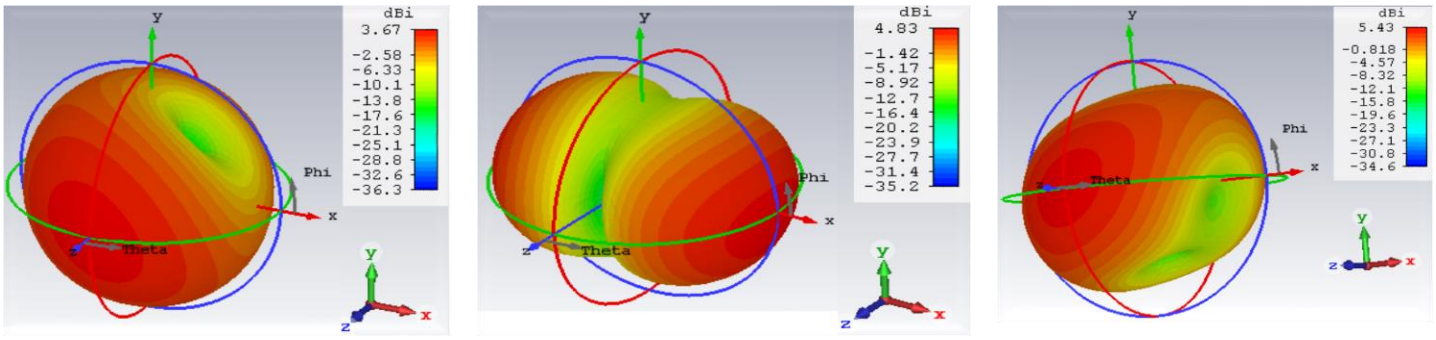

3.5 GHz 3.5 GHz 7 GHz

Separated N

Fig 6.21. Modal Far Field patterns for the Letter N.

The far field patterns simulated for both the antenna structures are pretty acceptable and can be useful for communication purposes for practical purposes.

6.6 MODE BANDWIDTH COMPARISONS OF THE ANTENNAS

The 3dB mode bandwidth of each of the antennas is compared. It is seen from the comparisons that many of the modes cover large frequency regions. Therefore, if fed properly, the antennas will be able to function as wideband antennas in the WLAN/ WiMAX regions.

Table 6.1

3dB mode bandwidth comparisons

Structure	Bandwidth of mode covering 2.5 GHz	Bandwidth of mode covering 3.5 GHz	Bandwidth of mode covering 5.2 GHz
Full A	No mode	1.12 GHz	2.1 GHz
Separated A	No mode	No mode	2.1 GHz
Full H	523 MHz	No mode	3.2 GHz
Separated H	No mode	No mode	3.8 GHz
Full M	No mode	500 MHz	No mode
Separated M	No mode	430 MHz	No mode
Full N	No mode	340 MHz	4.5 GHz
Separated N	No mode	Two modes present Mode 1-400 MHz Mode 2-600 MHz	4.2 GHz

6.7 CONCLUSION

Antennas resembling English alphabets have been designed in this paper. Characteristic Mode Analysis is used to find out the inherent modes and radiating nature of each such structure. The modal significance values of the resulting analysis are used to find out where the structures can potentially radiate.

The far-fields at these potential frequencies are simulated and presented. It can be seen that the expected radiating modes of the structures do indeed radiate and present acceptable radiation patterns in the far-field region.

The designed antennas can thus be used for wireless communication and they also cover some of the well known IEEE wireless standard communication channels like 2.5 GHz and 5.2 GHz (WLAN bands) as well as 3.5 GHz (WiMAX) band. The location and positions of the feeds can be determined by analyzing the electric field distributions of each associated mode at each frequency of interest. As seen from the table in the last section, the antennas if fed properly can act as wideband antennas.

REFERENCES

[1] R. J. Garbacz, "A Generalized Expansion for Radiated and Scattered Fields," Ph.D. dissertation, Ohio State University, Columbus, 1968

[2] R . J. Garbacz and R. H. Turpin, "A generalized expansion for radiated and scattered fields," *IEEE Trans. Antennas Propagation, vol. AP - 19, no. 3, pp. 348–358, May* 1971.

[3] R. F. Harrington and J. R. Mautz, "Theory of Characteristic Modes for Conducting Bodies," IEEE Trans. Antennas Propagation, vol. AP-19, no. 5, pp. 622- 628, Sept. 1971.

[4] R. F. Harrington and J. R. Mautz, "Computation of Characteristic Modes for Conducting Bodies," IEEE Trans. Antennas Propagation, vol. AP-19, no. 5, pp. 629- 639, Sept. 1971.

[5]Yikai Chen, Chao-Fu Wang**,** *Characteristic Modes: Theory and Applications in Antenna Engineering, John* Wiley and Sons, 2015.

CHAPTER - VII

CONCLUSIONS AND FUTURE PROSPECTS OF THE THESIS WORK

7.1 CONCLUSIONS

In the 3rd chapter, a simple printed dipole antenna with parasitic patches was designed having triple frequency characteristics. The proposed antenna is very simple to design and fabricate and has the advantage of being planar. The designed antenna shows good triple band resonance capabilities and a wide bandwidth in the 2.2GHz to 3.6GHz region with an added efficient resonance near 5.2 GHz due to addition of the parasitic patches. These are all standard IEEE wireless communication channels in the WLAN band and WiMAX band. The balanced feed ensures better operation of the structure as well as matching the antenna structure to the usual 50Ω port systems found in most cases.

In the 4th chapter, effects of two modified ground planes on the equilateral triangular ring shaped antenna have been studied and presented along with measured results. The antennas have been found to be wideband in nature, linearly polarized, omnidirectional and capable of covering some standard IEEE wireless communication channels like the WLAN band (2.5 GHz, 5 GHz) as well as the 3.5 GHz (WiMAX band) with good efficiency.

In the 5th chapter, a planar wideband star shaped patch antenna is presented with small size, good efficiency, linear polarization and omnidirectional patterns at 2.45 GHz (IEEE 802.11b/g/n, WLAN) and 3.5 GHz (IEEE 802.16d, WiMAX) which are standard IEEE communication channels. A central circular slot is added to the structure to enhance matching throughout the entire bandwidth.

In the 6th chapter, antennas resembling English alphabets have been designed in this paper. Characteristic Mode Analysis is used to find out the inherent modes and radiating nature of each such structure. The modal significance values of the resulting analysis are used to find out near what frequencies the structures can potentially radiate. The far-fields at these potential frequencies are simulated and presented. It can be seen that the significant characteristic modes of the structures radiate and present acceptable radiation patterns in the far-field region. The designed antennas can thus be used for wireless communication and they also cover some of the well known IEEE wireless standard communication channels.

7.2 FUTURE PROSPECTS OF THE WORKS

The antenna structure designed and fabricated in chapter 3 can be studied and modified further to reduce its size while retaining the triple band characteristics.

The modified ground plane effects of chapter 4 can be studied further with various ground plane shapes replacing the two used. Many new and useful properties might be found by changing the modified ground planes which might result in better optimized antennas. The triangular rings might also be fed in appropriate positions to get circular polarization which will enhance the usefulness of the antenna as receivers and transmitters.

The alphabet shaped antennas of chapter 6 need to be studied further. Following the current maximas and minimas of the various modes, the feed positions need to be placed accordingly and the simulations need to be run while including the feeds in either time domain or frequency domain in CST. The results need to be studied to observe the radiation efficiencies at the various resonances as well as the respective s11 matching at each frequency. The antennas might be fabricated after such simulations and tested in practical use.

LIST OF FIGURES AND TABLES

LIST OF FIGURES

CHAPTER 5

CHAPTER 6

LIST OF TABLES

PUBLICATIONS

1. Sayan Sarkar, Amartya Banerjee, Bhaskar Gupta, "*A Balanced Feed Triple Frequency Patch Loaded Printed Dipole Antenna for WiMAX/WLAN Application,"* 2018 IEEE International RF and Microwave Conference (RFM), Penang, Malaysia, December 2018. *****

2. Sayan Sarkar, Bhaskar Gupta, "*Characteristic Mode Analysis of a few Symmetric English Alphabet Shaped Antennas,"* URSI Asia Pacific Radio Science Conference (AP-RASC) 2019, New Delhi, India, March 2019. *****

***** Paper presented in conference, to be published in IEEE Xplore shortly.

3. Sayan Sarkar, Bhaskar Gupta, "*Effects of Two Different Modified Ground Planes on an Equilateral Triangular Ring-Shaped Patch Antenna*," 8th Asia-Pacific Conference on Antennas and Propagation (APCAP) 2019, Incheon, Korea. †

4. Sayan Sarkar, Bhaskar Gupta, "*A novel Star-Shaped Wideband Patch Antenna with Central Circular Slot for WLAN and WiMAX Applications,*" 8th Asia-Pacific Conference on Antennas and Propagation (APCAP) 2019, Incheon, Korea. †

† Paper accepted for oral presentation at APCAP 2019 (4th –7th August 2019.)